Submitted to Crystal Lattice Defects

RADIATION LABORATORY

UCRL-19680
Preprint c.2

DOCUMENTS SECTION

FIELD ION MICROSCOPE OBSERVATIONS ON PERITECTOID GROWTH OF Ni_4W

H. C. Tong and J. Washburn

June 1971

AEC Contract No. W-7405-eng-48

TWO-WEEK LOAN COPY

This is a Library Circulating Copy which may be borrowed for two weeks. For a personal retention copy, call Tech. Info. Division, Ext. 5545

LAWRENCE RADIATION LABORATORY
UNIVERSITY of CALIFORNIA BERKELEY

UCRL-19680 c.2

DISCLAIMER

This document was prepared as an account of work sponsored by the United States Government. While this document is believed to contain correct information, neither the United States Government nor any agency thereof, nor the Regents of the University of California, nor any of their employees, makes any warranty, express or implied, or assumes any legal responsibility for the accuracy, completeness, or usefulness of any information, apparatus, product, or process disclosed, or represents that its use would not infringe privately owned rights. Reference herein to any specific commercial product, process, or service by its trade name, trademark, manufacturer, or otherwise, does not necessarily constitute or imply its endorsement, recommendation, or favoring by the United States Government or any agency thereof, or the Regents of the University of California. The views and opinions of authors expressed herein do not necessarily state or reflect those of the United States Government or any agency thereof or the Regents of the University of California.

FIELD ION MICROSCOPE OBSERVATIONS ON PERITECTOID GROWTH OF Ni_4W

H. C. Tong and J. Washburn

Department of Materials Science
and Inorganic Materials Research Division
Lawrence Radiation Laboratory
University of California, Berkeley, California

ABSTRACT

Ni-20 at.% tungsten was successfully imaged and studied by field ion microscopy. The experiments show that two different mechanisms are involved in the peritectoid reaction, a homogeneous disorder → order transformation, $\alpha \rightarrow \beta$ takes place in the α phase at lower temperatures, but the mechanism is nucleation and growth of β phase involving long range diffusion of tungsten at higher temperatures. The results suggest that below 800°C the range of stability of the ordered β phase extends below 37 wt.% tungsten. It was also found that some long range order with a domain size of approximately 50 - 100Å still existed in the α phase when the alloy was annealed for 9 hours at 1300°C and quenched to room temperature.

The defects and substructure resulting from the ordering process are discussed. A correspondent matrix was derived which can be used to determine the conditions under which an antiphase boundary will not be visible on a field ion image.

I. INTRODUCTION

The mechanism of growth of Ni_4W was studied by Epremian and Harker.[1] Their x-ray observations suggested that the mechanism of formation of the ordered β phase was different at low and high temperatures. Ordinary nucleation and growth of nearly stoichiometric β with gradual disappearance of γ and α phases took place at 950°C aging temperature whereas a disorder to order reaction in the α phase took place at aging temperatures below 750°C. Their results also showed that the range of stability of the β phase below 850°C should extend at least as low as 17.6 at % W.

Field ion microscopy is capable of providing very direct information concerning the mechanism of phase transformations. Because order-disorder transitions require only local atomic rearrangement, no long range diffusion, microscopic observations on the atomic scale are necessary for studying the mechanism. Field ion microscopy provides the required resolution, but to date only a few systems such as Pt-Co,[2,3,4] and Ni_4Mo[5] have been successfully studied by this technique.

In general, different types of antiphase domain boundaries are formed as a result of ordering. Substructures in ordered phases have been studied by electron microscopy and analytically, but not much by field ion microscopy. To the authors' knowledge the F.I.M. image and the substructure of Ni_4W have not previously been investigated.

Structure of Ni_4W

The constitution diagram of the Ni-W system has been studied by many investigators. Epremian and Harker were the first to show that Ni_4W forms a superlattice derived from the FCC structure. Ordering results

in a slight distortion to a tetragonal symmetry with $c_o/a_0 = 0.980$. The phase diagram published by Ellinger and Sykes[6] is shown in Fig. 1.

The ordered β phase has a body centered tetragonal unit cell containing two W atoms and 8 Ni atoms. The relationship between the Ni_4W unit cell and the distorted FCC lattice is shown in Fig. 2. Based on the crystallographic arrangement shown in Fig. 2 the relationship can be algebraically represented by a matrix equation

$$A_o = \beta_{oi} P_1 A_i \quad \ldots\ldots\ldots\ldots \quad (1)$$

where $A_o = \begin{pmatrix} h \\ k \\ \ell \end{pmatrix}$ is a vector formed with the Miller indices based on the distorted FCC lattice $A_i = \begin{pmatrix} H \\ K \\ L \end{pmatrix}$ is the vector formed with indices based on the unit cell Ni_4W, $P_1 = \frac{1}{5}\begin{pmatrix} 3 & 1 & 0 \\ -1 & 3 & 0 \\ 0 & 0 & 5 \end{pmatrix}$ is a transformation matrix and

$$\beta_{oi} = \sqrt{(h^2 + k^2 + \ell^2)/(H^2 + K^2)\frac{2}{5} + L^2)}$$

The above matrix is not unique, but depends on how the ordering process starts with respect to the disordered α phase. An ordered domain can be formed in six different orientations for a given orientation of original FCC matrix, furthermore, there are five equivalent translational positions for an ordered domain. This results in thirty ways of forming equivalent ordered domains. Fig. 3 shows the six different ordering orientations.

If we choose the geometrical relationship shown in Fig. 2 as our standard ordering sense, and let P_1 represent the relationship between the distorted FCC cell and the Ni_4W cell, then the mathematical relationship between other equivalent Ni_4W cells with respect to the fixed orientation of the disordered phase can be expressed by matrices,

P_i (i = 1, ... 8), i denotes the type of ordering according to Fig. 3, where

$$P_1 = \frac{1}{5}\begin{matrix} 3 & 1 & 0 \\ -1 & 3 & 0 \\ 0 & 0 & 5 \end{matrix}$$

$$P_2 = \frac{1}{5}\begin{matrix} -1 & 3 & 0 \\ 3 & 1 & 0 \\ 0 & 0 & -5 \end{matrix}$$

$$P_3 = \frac{1}{5}\begin{matrix} 0 & 0 & 5 \\ -1 & 3 & 0 \\ -3 & -1 & 0 \end{matrix}$$

$$P_4 = \frac{1}{5}\begin{matrix} 0 & 0 & -5 \\ 3 & 1 & 0 \\ 1 & -3 & 0 \end{matrix}$$

$$P_5 = \frac{1}{5}\begin{matrix} 3 & 1 & 0 \\ 0 & 0 & 5 \\ 1 & -3 & 0 \end{matrix}$$

$$P_6 = \frac{1}{5}\begin{matrix} -1 & 3 & 0 \\ 0 & 0 & -5 \\ -3 & -1 & 0 \end{matrix}$$

In this paper some F.I.M. observations on Ni_4W are presented which further demonstrate the usefulness of field ion microscopy in the study of phase transformations.

II. EXPERIMENTAL PROCEDURE

An ingot of Ni-20% at. W was prepared by melting 99.95% pure nickel and G.E.218 tungsten wires together in an argon arc furnace. This ingot was then cut into small pieces and melted twice for better mixing. The final treatment was to anneal the ingot in a vacuum furnace for 90 hours at 1300°C and then quench into oil at room temperature. The ingot was then swaged into a 0.01 in. wire. Several intermediate anneals were necessary during the swaging process. The wires were aged at 1300°C for 9 hours and were quenched in oil at room temperature. We will refer to the alloy in this condition as the as quenched alloy.

The ordering temperature for Ni_4W is 970°C ± 10°C. Ordered and partially ordered wires were prepared by annealing the as quenched alloy wires in small evacuated quartz tubes at various temperatures below this critical temperature. At the end of the ordering heat treatment the wires were quenched into water at room temperature.

Field ion tips were prepared from the wires by standard electropolishing techniques. Pure helium from a container of liquid helium was used to cool the field ion tip so that the tip temperature could be controlled by the flow rate of the cold gas.

III. RESULTS AND DISCUSSION

3.1 Field Ion Image of As quenched Alloys:

Figure 4 shows a field ion micrograph of an as quenched alloy which was annealed at 1300°C for 9 hours in a vacuum furnace and was quenched into oil directly. Because more than 90% of the volume of the as quenched alloy is α phase of approximately 38 wt.% W and the particles of W rich solid solution are distributed through the α matrix in a coarse dispersion, only the α phase is usually observed in a FIM tip. The field ion image of the α phase frequently has a <111> direction near its center or less frequently <100> as a result of the preferred orientation developed during drawing of the wires.

The field evaporation characteristics of this as quenched α solid solution are sensitive to temperature. The field evaporation voltage is very close to the best imaging voltage when the tip temperature is at liquid nitrogen temperature, and a slow evaporation process still goes on at the best imaging voltage. The ion image becomes more stable only when the tip is developed to a larger size which usually

corresponds to a tip voltage of about 15 kV.

The tip end form after field evaporation is also sensitive to the temperature. When the field ion tip is developed at liquid nitrogen temperature, the field ion image showed bright clusters scattering all over the tip surface. Figure 5 shows a typical image. With a tip developed near liquid helium temperature the end form showed a much more even surface; the scattered clusters disappeared (Fig. 4).

The low index plane ring patterns of the cubic structure can still be recognized. The spots on this pattern can be roughly separated into two groups, bright and dim. It seems likely that both tungsten and nickel atoms are contributing to the image.

Many incomplete ring patterns and certain well developed planes which do not correspond to very low index planes of the f.c.c. lattice can be found in the image. Some of these planes are indicated by circles in Fig. 4. They are $\{210\}_{fcc}$. In addition, the occurence of half rings is frequent compared with the computer simulation of a completely disordered Ni - 20% at. W alloy (Fig. 6). The computer simulation shown in Fig. 6 was derived from the f.c.c. computer image shown in Fig. 7 by assuming that only one fifth of the spots chosen at random will appear.

Many dark lines were observed in the as quenched field ion images. Frequently, a string of bright imaging spots decorated these dark lines. These lines divide the entire image into many small divisions, each division being about 50 - 100Å in size. They can be brought out with

better definition if the photograph is taken while slow field evaporation is going on as shown in Fig. 8.

3.2 The Image of Fully Ordered Ni_4W:

A fully ordered Ni_4W field ion micrograph is shown in Fig. 9. The image is stable even when the tip is at liquid nitrogen temperature as long as the imaging voltage is over 15 kV. When the tip temperature is cooled by liquid helium, the whole image becomes extremely stable.

Since W atoms contribute the major image spots, only one fifth of the total ionization emission centers are effective and consequently the imaging gas pressure required for imaging Ni_4W is much less than that for a tungsten tip to produce approximately equal brightness at the same voltage. For example, only 1 to 2 x 10^{-4} torr is needed for imaging Ni_4W at 12 kV while, for most cases, a pressure of 10^{-3} torr is needed for imaging tungsten.

The field evaporation rate of Ni_4W is very sensitive to temperature, the gap between the best imaging voltage and the field evaporation voltage is very small at liquid nitrogen temperature, but is large at liquid helium temperature, for example, at 15 kV the gap is 0.5 to 1.0 kV at liquid nitrogen temperature, while at liquid helium temperature, the gap is about 2 to 2.5 kV.

The field ion micrograph shown in Fig. 9 is indexed according to a body centered tetragonal unit cell. A stereographic projection of the b.c.t. structure for Ni_4W was calculated, Fig. 10, and was used to index the micrograph. It is easy to see that the overall symmetry of the field ion micrograph is the same as the symmetry shown in the stereographic projection.

There are two ways to orient the β phase with respect to each {100} axial direction of the parent f.c.c. phase. To determine which of the two ways the ordered domain of Fig. 9 was formed it is necessary to distinguish which planes are fundamental planes and which are superlattice planes among the {121} family.

The contrast of the ring pattern is much more uniform and brighter for a superlattice plane because there is only one kind of atom in each individual layer. In Fig. 4 plane (121) is the fundamental plane and plane (211) is the superlattice plane. The planes can also be distinguished if a twin boundary cuts across a {211} plane; if no disruption of the pattern occurs near a particular {211} pole then it must be a fundamental plane.

For most binary alloys only one atomic species produces imaging spots. For example, assuming invisibility of Co atoms in Pt-50% at. Co alloy, Tsong and Müller[2] were able to give reasonable interpretations of the atomic packing on (001) planes of the P_t-Co ordered phase. In the Ni_4Mo system, Hren[4] concluded that only Mo atoms contribute imaging from a comparison of the tip radii obtained by ring counts on the layered planes and from the equation, $R = \frac{V^4}{5r}$. We propose another convincing way to show that only W atoms produce major imaging spots: For the Ni_4W structure, the {121} family has two subfamilies. One is the set of fundamental planes and the other is the set of superlattice planes. The interplanar spacing of the fundamental planes is five times that of the superlattice planes. Therefore, for an approximately spherically shaped field ion tip, the ring counts away from the poles of {121} subfamilies for a fixed arc length should be

different. Only three cases can occur, if both atomic species produce imaging spots, then the ring counts for the superlattice plane should be five times that of the fundamental planes, if only Ni atoms image, the ring counts for the superlattice plane should be 4 times that for fundamental planes.

If only W atoms produce the major imaging spots equal rings counts should be observed for both subfamilies. In Fig. 9 one of the planes (121) and (211) must be a fundamental plane and the other is a superlattice plane. It is clear that the ratio of ring counts is close to 1. Therefore, only W-atoms produce major imaging spots. The good fit of the field ion image pattern to the stereographic projection of a b.c.t. structure further supports this conclusion.

3.3 Partially Ordered Alloys:

3.3.1. Alloys aged at 750°C:

A F.I.M. micrograph of the alloy aged for one hour at 750°C is shown in Fig. 11(a). The micrograph shows almost the same characteristics as that of the as quenched alloys. Many random spots and a lot of incomplete half ring patterns can be seen. Low index planes can be recognized quite easily by their higher density of packing. Numerous dark lines similar to those seen in the as quenched alloy also appear at this stage as shown in Fig. 11(b).

At a few places, one indicated by arrow in Fig. 11(a), there is a more regular arrangement of atomic packing. These places do not correspond to planes of high atomic population for the f.c.c. structure. Therefore, we believe that it is a sign that localized regions have become ordered at this temperature.

3.3.2. Alloy aged at 850°C:

A F.I.M. image for the alloy aged at 850°C for 30 minutes showed clearly that ordering had developed at numerous centers over the entire region of the specimen. Each individual domain can be distinguished, and the average domain size is approximately 50 ~ 100Å. For each small domain ordering has reached an advanced stage. (See Fig. 12(a) and 12 (b)).

Because the domain size is so small, it is completely impossible to index the F.I.M. micrograph. Field evaporation frequently tended to strip away small pieces of the tip material rather than to strip one atom after another. Therefore, many of these tips were lost during observation. Because no regions of disordered α phase were observed the range of stability of the ordered β phase must extend at least as far as 38 wt.% W on the low tungsten side. This observation confirms the x-ray results of Epremian and Harker.[1]

3.3.3. Alloys aged at 920°C:

The peritectoid temperature for this alloy is 970° ± 10°C. Fig. 13(a) shows a F.I.M. micrograph of an alloy aged at 920°C for only 18 minutes. Both ordered β phase and disordered α phase regions were found co-existing together. The ordered domains within the α were much larger than those formed during annealing at 850°C. Some of the β phase regions touched each other, and some of them were separated by α phase regions.

When the annealing time was increased, the ordered β phase regions became larger and more of them came into contact with each other, but some α phase volume still remained. In Fig. 13(b), the area inside

the dashed line is still an α phase region. In the β phase many vertically elongated domains can be seen. These domain boundaries could be accentuated by making the exposure while a very slow field evaporation was going on, [Fig. 13(c)]. We believe that these boundaries are formed by dislocations which are moved under the action of the extremely high stress associated with the electrostatic field. Particularly when a tip is ellipsoidal there are shear components. The slip system for this plastic flow is still not clear. A similar phenomenon has also been observed in the pure metals iridium[7] and cold worked tungsten.

When the annealing time was increased to 3 hours, the ordered domains became very large. α and β phase regions were very clearly distinguishable (Fig. 14). Within each β particle long range order was almost perfect. At this temperature the formation of β was clearly a nucleation and growth process involving solution of γ phase particles and diffusion of W to the advancing β-α interface. In the alloy annealed for 90 hours at this temperature the β phase regions were large enough to occupy the entire FIM tip. Each β phase grain was composed of very large domains.

4. Defects in the Ordered Structure:

4.1. Point Defects:

Three kinds of elementary point defects can occur in an ordered alloy, they are vacancies, interstitials, and misplaced atoms. In Fig. 15 some very weak image spots can be seen among the bright edge of superlattice planes. Two of them are indicated by open arrows. By comparing the frequency of appearance of these weak imaging spots

to the known concentration of impurities it was concluded that they are most likely due not to impurities but rather to misplaced Ni atoms. The Ni-layers in the superlattice plane are extremely unstable on exposure to the imaging field. Occasionally we were able to see a very faint Ni ring, but when a nickel atom is on a tungsten site the surrounding W. atoms may shield a portion of the field and consequently the Ni atom becomes stable enough to remain. For the same reason, the Ni atoms along a fundamental plane edge are also more stable than Ni atoms in a layer populated entirely by nickel.

Tungsten atom vacancies were also found in the field ion micrographs as would be expected in β phase of composition less than 43 wt.% W. They appear as completely dark sites in a superlattice plane. One of them is indicated by a circle in Fig. 15.

During the observation period some extra bright spots occasionally appeared in the central position of certain superlattice planes. These could have been misplaced tungsten atoms in Ni layers.

4.2. Translational Antiphase Boundaries and Line Defects:

A perfect superdislocation can dissociate itself into partial dislocations. These partial dislocations are associated with stacking faults or translational antiphase boundaries. Le Fevre, et al.[8] have discussed the application of the (g.R) criterion[9] to the contrast of translational antiphase boundaries in ordered Ni_4Mo field ion images. They showed that if (g.R) ≠ integer (where g is the reciprocal lattice vector of the plane and R is the displacement vector for the antiphase boundary) the translational antiphase boundaries in an ordered Ni_4Mo field ion image will give contrast in the form of a mismatching of the

ring patterns along the boundary.

A loop of partial dislocation is indicated in Fig. 16 and the mismatching of the ring pattern is clear. Figure 17 shows another case of a partial which causes a trace of mismatch across the (110) plane. A perfect superdislocation has not been found in our field ion micrographs.

4.3. Domain Structure:

The interface between two different ordered domains which have nucleated from a common parent grain of perfect single crystal is an antiphase boundary. Only certain relative orientations are possible. If we define the three axes of the ordered structure with respect to the three axes of the parent disordered crystal as shown in Fig. 2, then the orientation relationship between any two domains nucleated from the common single crystal grain can be represented by a matrix. Eq. 2 shows the algebraic relationship between any two domains of type i and j:

$$A_i = \gamma_{ij}\, C_{ij}\, A_j \qquad \gamma_{ij} = \frac{(\sqrt{h^2 + k^2)\frac{2}{5} + \ell^2})i}{(\sqrt{h^2 + k^2)\frac{2}{5} + \ell^2})j}$$

and $C_{ij} = P_i^{-1} P_j$

where A_i, A_j are vectors formed with the Miller index of the ith and jth domain respectively. P_i^{-1} is the inverse of the transformation matrix P_i. The case i = j is a trivial one which corresponds to two ordered domains separated by a translational antiphase boundary.

Except for the simplest form of translational antiphase boundary the others can be classified as antiparallel twin, perpendicular twin

and complex boundaries. In general, the above antiphase boundaries are formed either by simple lattice translation, pure rotation or by the combination of both.

The matrix of correspondence can be used in the analysis of the substructures resulting from the ordering process. From the matrix of correspondence, it can be shown that for any two neighboring domains there is a set of correspondent pairs of planes which belongs to the same family which corresponds to the same plane in the disordered phase. It should be noticed that each pair consists of either fundamental planes or superlattice planes, there are no mixed pairs. In this paper we will refer to these pairs of planes as congruent planes. The low index congruent planes for the antiparallel twin and the perpendicular twin can be found from Eq. 2.

The field ion image of an ordered alloy which consists of several domains can be analyzed much more easily with the aid of the matrix of correspondence.

Usually the field ion tips are made from materials which have been drawn into wires or made from strips cut from a sheet. Field ion microscope specimens of ordered alloys can be prepared by heat treatment of the as quenched wires or strips. Once the preferred orientation of the disordered wire is known by indexing of the field ion image or from an x-ray pole figure then the likely axial directions of an ordered alloy can be calculated from the transformation matrix and hence the possible graphic stereographic projections of the ordered structure can be constructed. The major domain in the field ion micrograph is then indexed. The possible corresponding axial directions

C_i of its neighbor domain can then be calculated by Eq. 2. Superposing the two stereographic projections by matching the axial directions and their congruent planes, the neighbor domain can then be indexed, and the relationship of this domain with respect to the major domain is then determined.

The contrast in the field ion image of a domain boundary is due to the mismatch of the ring patterns. However, when a domain boundary passes a congruent plane, there is no mismatch of the ring patterns, and hence no field ion contrast can be observed unless the domain boundary is of the complex type or is a translational antiphase boundary which passes a superlattice congruent plane.

Figure 18,AA shows an antiparallel twin boundary cutting through the congruent plane $(12\bar{1})//(121)$ and $(2\bar{1}\bar{1})//(\bar{2}11)$. These planes are fundamental planes according to crystallography. As expected, no field ion contrast can be found near these two planes. Figure 19 shows the corresponding stereographic projection of this field ion tip.

DISCUSSION

5.1. The domain structure in the as quenched alloy:

The α phase quenched from 1300°C showed numerous dark lines. These dark lines intersected themselves and formed many small regions of 50 ~ 100Å diameter. They are shown with greater clarity in Fig. 8 which is a micrograph taken during slow field evaporation. By this method, any possibility that the lines might be due to accidnetal arrangement of surface atoms is rule out. Also, some well arranged atomic planes which are indicated by circles in Fig. 3 were frequently found in $\{210\}_{fcc}$ planes which do not correspond to the most dense planes

in the f.c.c. structure but do correspond to the most prominent superlattice planes $\{110\}_{bct}$.

Because the as quenched alloy had been annealed at 1300°C for 9 hours before quenching to room temperature, the dark lines in the α phase are unlikely to be stacking faults. They also cannot be grain boundaries because the relative positions of the most prominent planes can be indexed on the pattern and are at their proper positions. The only reasonable conclusion is that the α phase, when it is quenched from 1300°C, attains some degree of long range order with the approximate domain size of 50 ~ 100Å.

As indicated in Fig. 8, some of these boundaries which were found in as quenched alloys were clearly distinguishable in one place, but tended to disappear at nearby positions. The boundaries did not form an interconnected network but rather tended to be fragmentary.

5.2. The mechanism of ordering:

Recently Newman and Hren studied Ni_4Mo[4] and concluded that the ordering mechanism is a homogeneous reaction, Okamoto[13] found the early stages of ordering of the alloy Ni_4Mo aged at 650° and 750°C were characterized by bright, well defined planes or groups of atoms about the <420> matrix poles. He interpreted this as an indication of composition fluctuations. In the same period, Saburi[11] reported results on Ni_4Mo and concluded that the transformation of Ni_4Mo follows nucleation and growth of long range ordered domains in the short range ordered matrix. Ni_4W has the same structure as Ni_4Mo in the ordered structure. Epremian and Harker studied Ni_4W by x-ray diffraction[5] and reported that there are two possible mechanisms by which Ni_4W might form,

each having different characteristic sequences of diffraction patterns.

Our results show that ordering starts just above 750°C as shown in Fig. 11(a) in agreement with the results obtained by Epremian and Harker. When the alloy was annealed at 850°C for 30 min. the whole specimen was filled with small domains with an averaged size 50 ~100Å as shown in Fig. 12(b). This size is quite close to that of the domains that were partially bounded by fragmentary domain boundaries in the as quenched alloy. Each of these very small domains seems to have reached a quite advanced stage of long range order even though the composition of the α phase is quite far from the ideal 20 at.% W. When the alloy was annealed at 920°C, the ordering mechanism was different. Long range order nucleated only at a few places. The ordered domains grew slowly into the disordered α matrix, eventually becoming very large. The sequence of annealing at 920°C can be seen in Fig. 13(a), 13(b), 13(c). Finally when the annealing time was sufficiently long the entire volume of a F.I.M. tip became a single domain of ordered β phase as shown in Fig. 9.

We conclude that the mechanism of ordering for Ni_4W is a homogeneous reaction at low temperature, with domain size and the sense of each domain being predetermined during quenching, but at high temperature the mechanism is nucleation and slow growth of long range ordered β phase domains into the disordered α matrix involving diffusion of W to the α-β interface and solution of tungsten rich γ phase particles.

CONCLUSIONS

1. Ni_4W can be imaged sucessfully and can be used to study an order-disorder transformation by F.I.M., W-atoms are the major imaging atomic species.
2. A certain degree of long range order with a domain size approximately 50 ~ 100Å exists in the α phase even just after the alloy has been quenched from 1300°C.
3. Growth of ordered β phase from the quenched two phase Ni 20 at.% W alloy is different at low and high aging temperatures. At low temperatures a homogeneous ordering reaction occurs within the α phase even though the W content is well below 20 at.%. The size and orientation of domains being pre-determined during the quench. At higher temperatures, there is nucleation and slow growth of β phase within the disordered matrix of a few perfectly ordered domains. Because nucleation occurs only at a few centers, probably at the interface between α and γ phases, the domains are very large when they eventually grow into contact.

REFERENCES

1. E. Epremian and D. Harker, Trans. AIME, 185, 267 (1949).
2. T. T. Tsong and E. W. Muller, Appl. Phys. Letters 9, 7 (1966).
3. T. T. Tsong and E. W. Muller, J. Appl. Phys. 38, 5451 (1967).
4. H. N. Southworth and B. Ralph, Phil. Mag. 14, 383 (1966).
5. R. W. Newman and J. J. Hren, Phil. Mag. 16, 211 (1967).
6. F. H. Ellinger and W. P. Sykes, Trans. ASM 28, 619 (1940).
7. E. W. Muller and T. T. Tsong in Field Ion Microscopy (American Elsevier Publishing Company, Inc. 1969) p. 263.
8. B. G. LeFevre, H. Grenga and B. Ralph, Phil. Mag. 18, 1127 (1968).
9. S. Ranganathan, H. B. Lyon, and G. Thomas, J. Appl. Phys. 38, 4957 (1967).
10. P. Okamoto, Ph. D. Thesis, University of California, 1970.
11. T. Saburi, K. Komatsu and S. Nenno, Phil. Mag. 20, 1091 (1969).

FIGURE CAPTIONS

Fig. 1. The phase diagram of the Ni-W system.

Fig. 2. View of the structure of Ni_4W along $[001]_{fcc}$, showing the relationship between the small f.c.c. unit cell and the larger b.c.t. unit cell of the ordered structure.

• : Ni atoms in the first (001) layer

● : W atoms in the first (001) layer

o : Ni atoms in the next (001) layer

o : W atoms in the next (001) layer

Fig. 3. The six different orientations of the ordered crystals relative to the disordered matrix.

Fig. 4. The field ion micrograph of an as quenched alloy which was annealed at 1300°C for 9 hours in vacuum and then quenched into oil. The densely packed planes $\{210\}_{fcc}$ are indicated by circles.

Fig. 5. A typical field ion image when the tip is at liquid nitrogen temperature.

Fig. 6. A computer simulation of a $[001]_{fcc}$ oriented F.I.M. image of a completely disordered Ni-20% at. W alloy assuming that only $\frac{1}{5}$ of the spots shown in Fig. 7 are imaged. The remaining spots were chosen at random.

Fig. 7. Computer simulation of a $[001]_{fcc}$ F.I.M. image of a crystal having the f.c.c. structure.

Fig. 8. Field ion photograph of as quenched alloy which was taken while a slow field evaporation was going on. Note the numerous dark lines.

Fig. 9. A fully ordered Ni_4W field ion micrograph.

Fig. 10. The stereographic projection of the ordered structure for comparison with the field ion micrograph shown in Fig. 9.

Fig. 11. F.I.M. micrographs of a partially ordered alloy aged at 750°C.

a) Aged for one hour at 750°C

b) Same as a) except that the micrograph was taken while slow field evaporation was going on.

Fig. 12. F.I.M. micrographs of a partially ordered alloy aged at 850°C for 30 minutes.

a) Micrograph taken at liquid nitrogen temperature for better definition of antiphase boundaries.

b) Micrograph taken at a lower temperature for better point resolution.

Fig. 13. The partially ordered alloy aged at 920°C.

a) Aged for 18 minutes

b) Aged for 30 minutes

c) Same as 13b except that the micrograph was taken while slow field evaporation was going on.

Fig. 14. F.I.M. micrograph of an alloy aged at 920°C for 3 hours.

Fig. 15. Point defects in ordered Ni_4W: A tungsten vacancy is indicated by a circle, the weakly imaged spots indicated by open arrows are most likely misplaced Ni atoms in the tungsten sublattice, and a bright spot indicated by an arrow is likely to be a misplaced W atom in a Ni sublattice.

Fig. 16. A shockley partial loop causing mismatching of the ring pattern is shown in this micrograph.

Fig. 17. A partial dislocation causing a trace of mismatch across a (110) plane.

Fig. 18. An antiparallel twin boundary indicated by A-A. Note that where this boundary passes the congruent plane $(12\bar{1})//(121)$ and $(2\bar{1}\bar{1})//(\bar{2}11)$ the ring mismatch disappears.

Fig. 19. Stereographic projection corresponding to the field ion micrograph shown in Fig. 18.

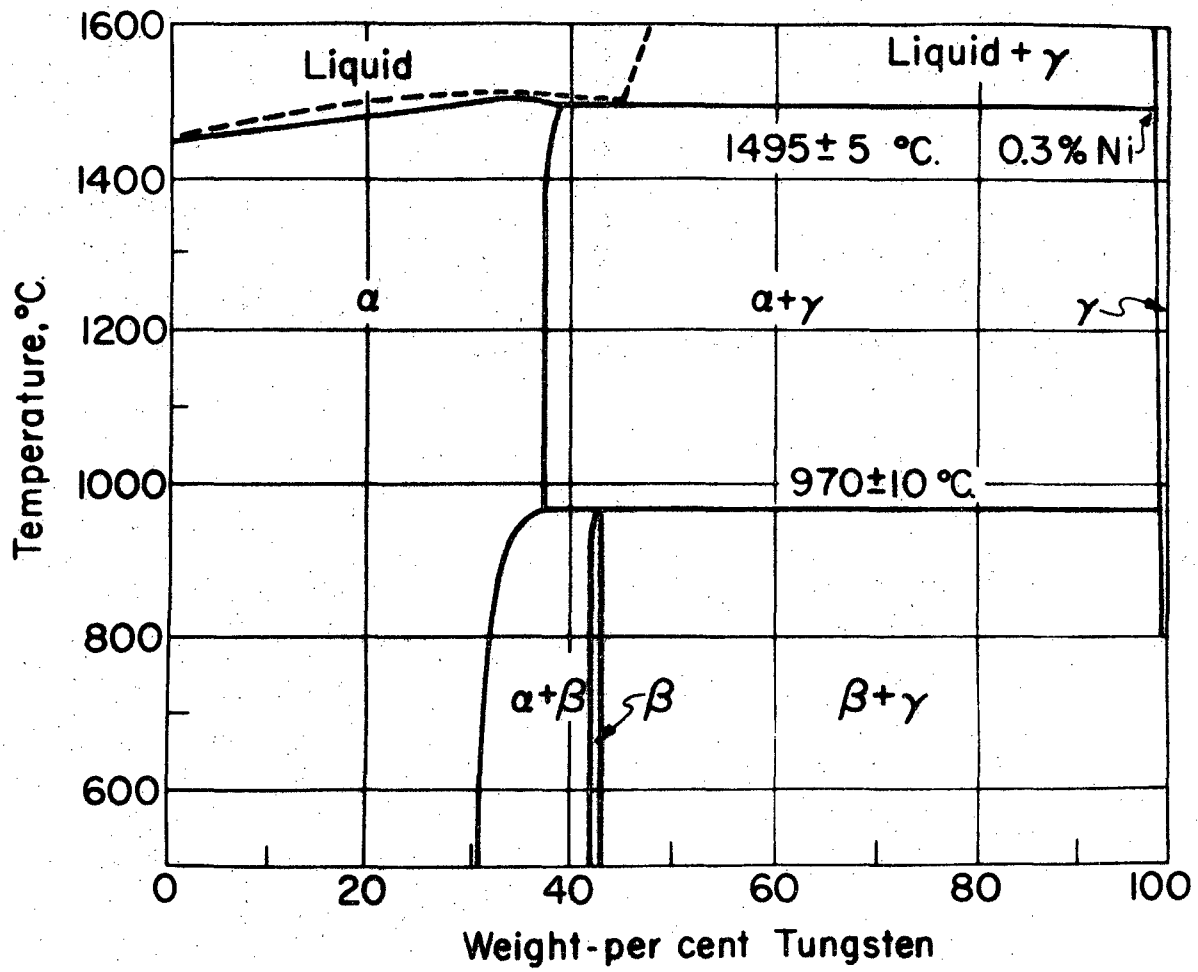

XBL 7010-6707

Fig. 1

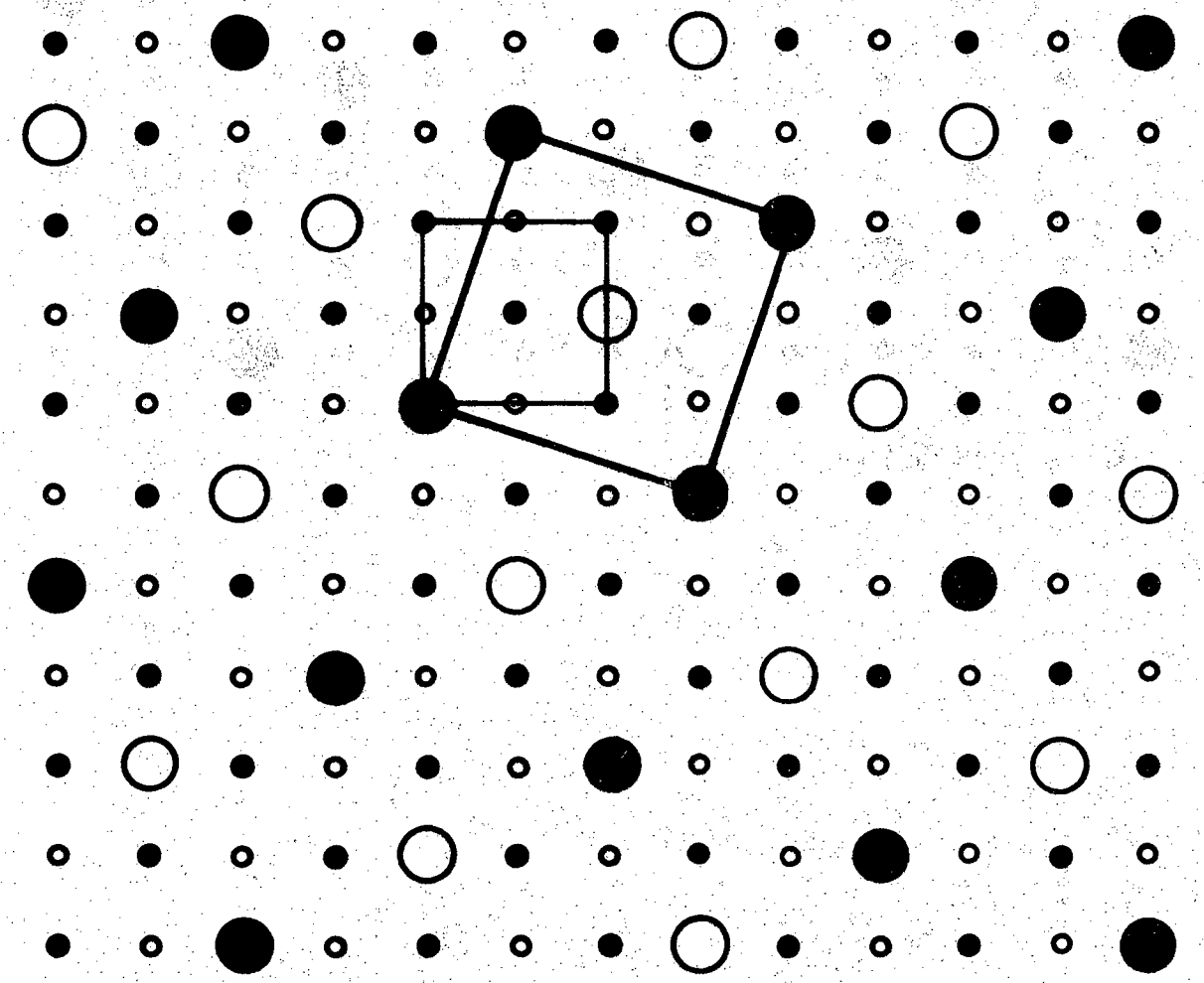

XBL708-3624

Fig. 2

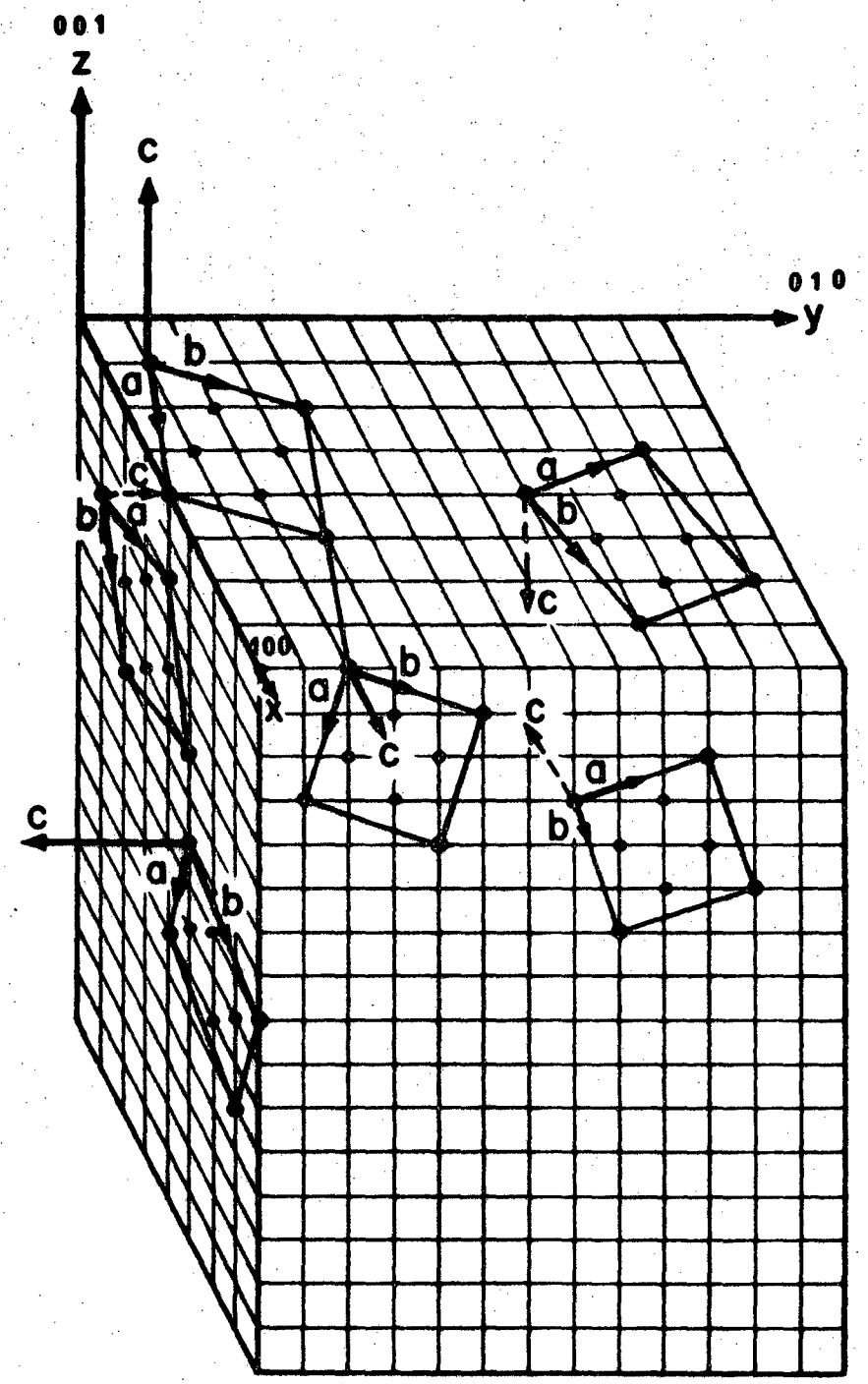

XBL708-3622

Fig. 3

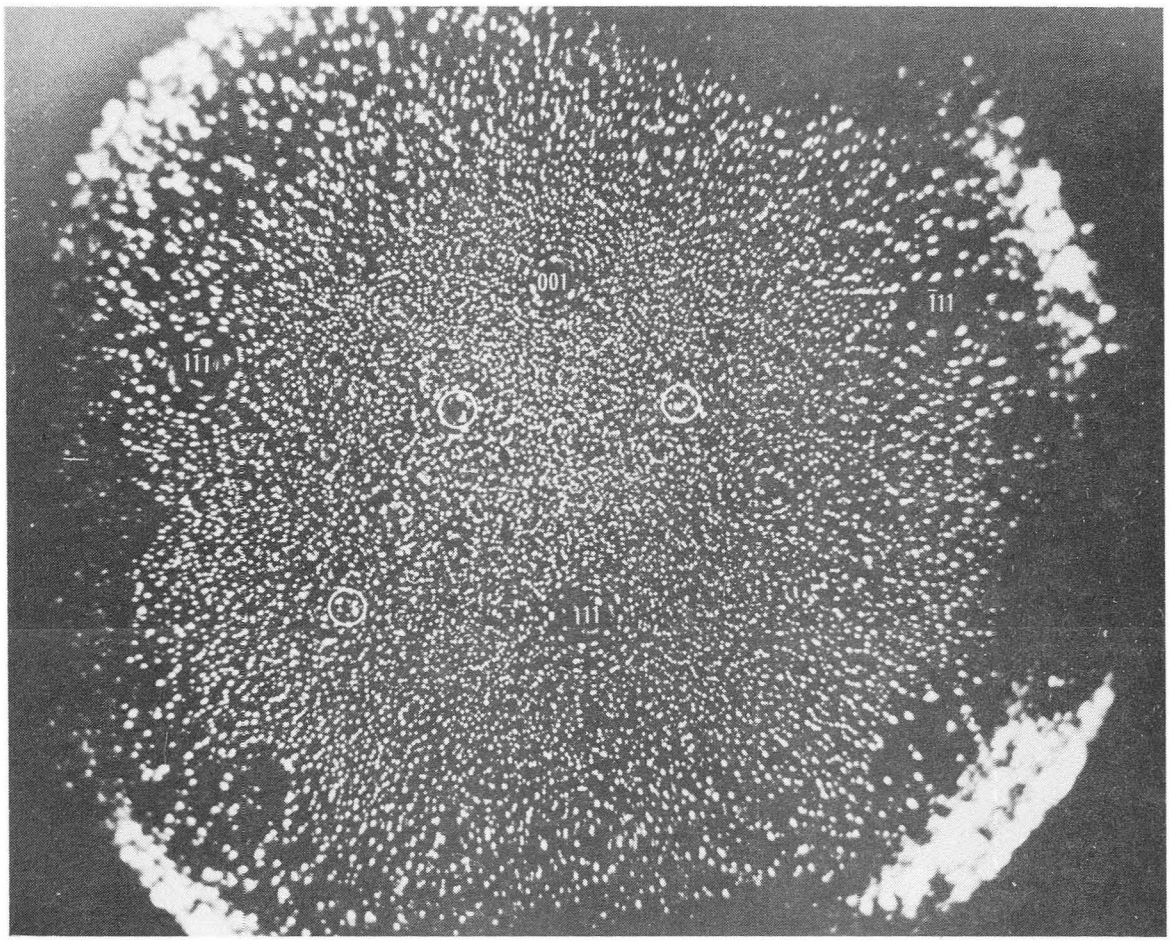

XBB 715-2318

Fig. 4

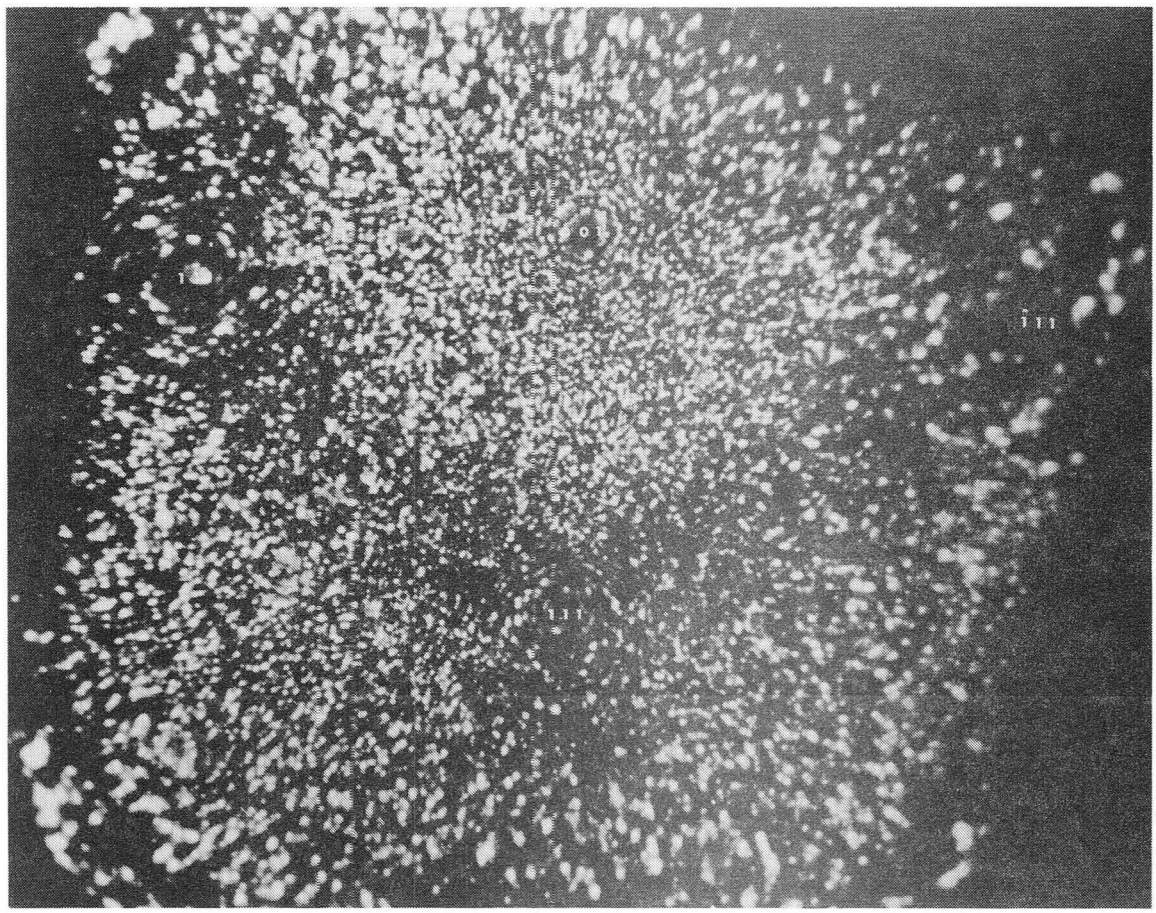

XBB 715-1888

Fig. 5

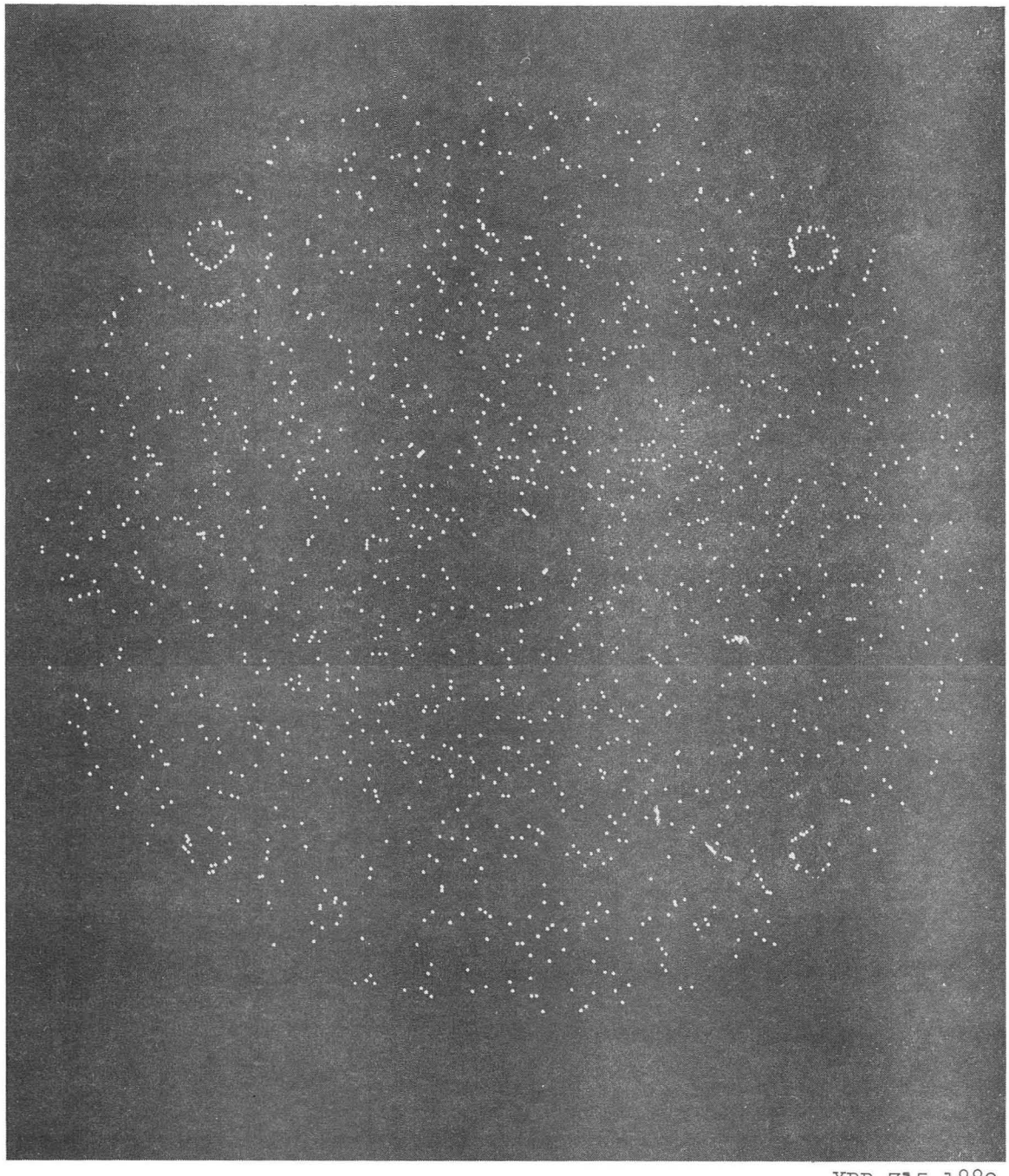

XBB 715-1889

Fig. 6

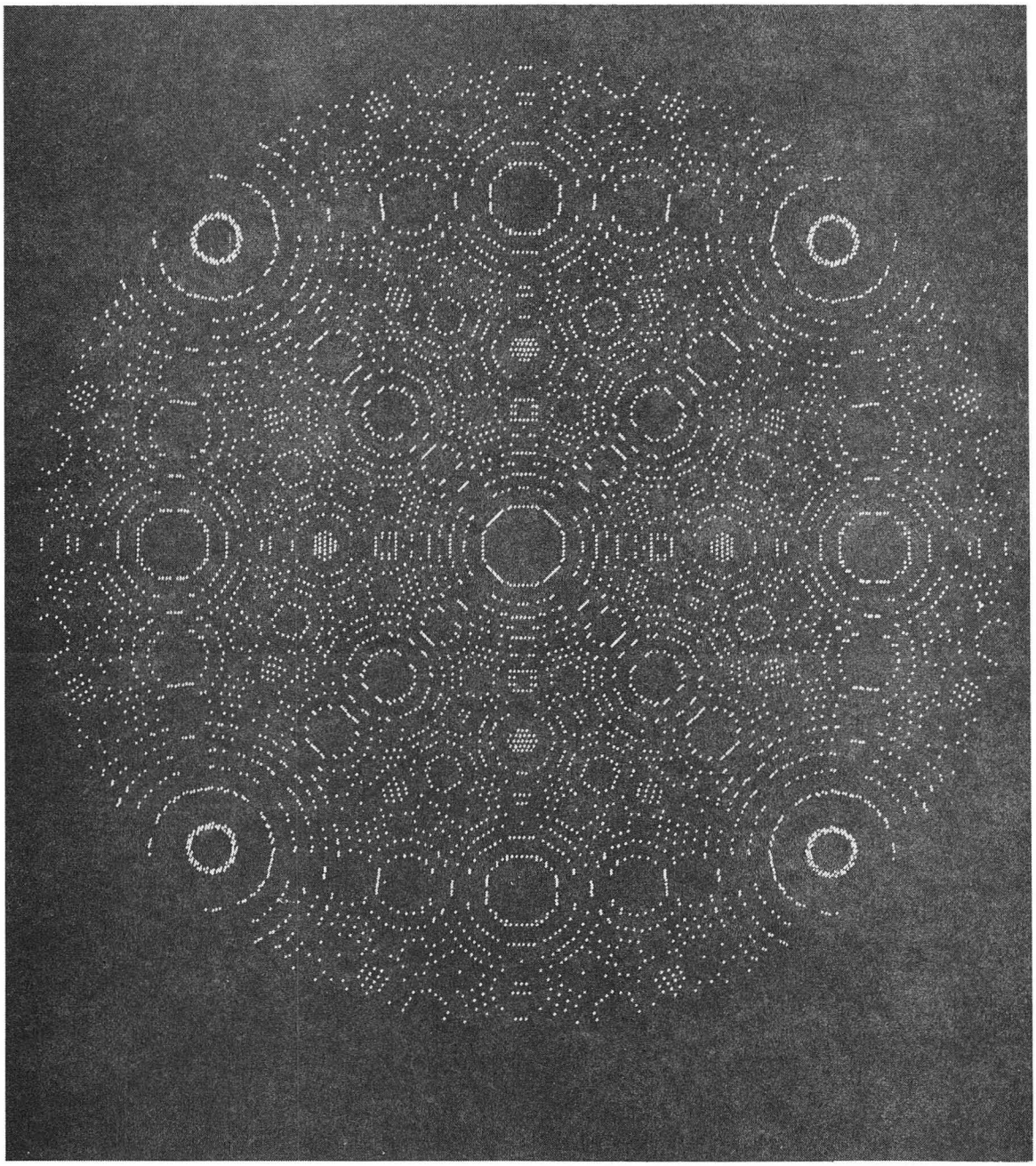

XBB 715-1888

Fig. 7

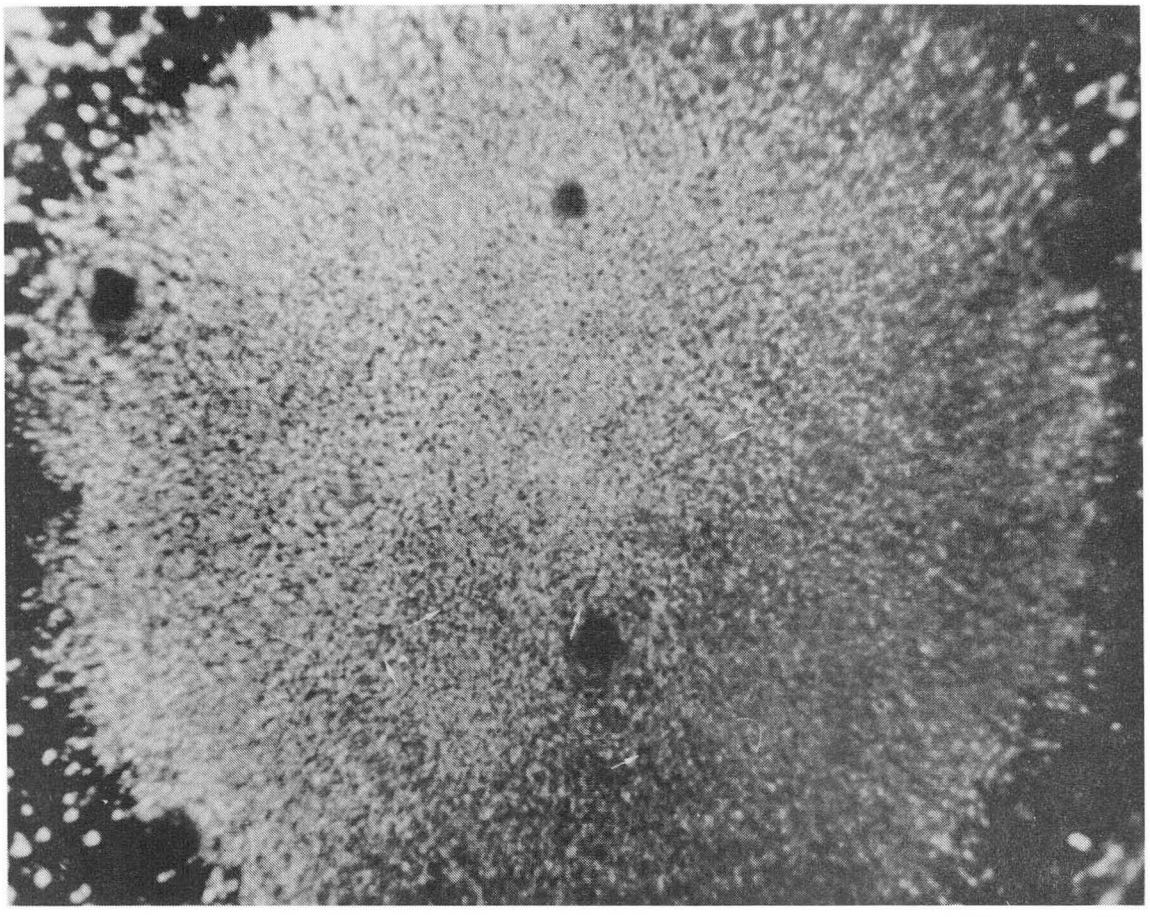

XBB 715-1882

Fig. 8

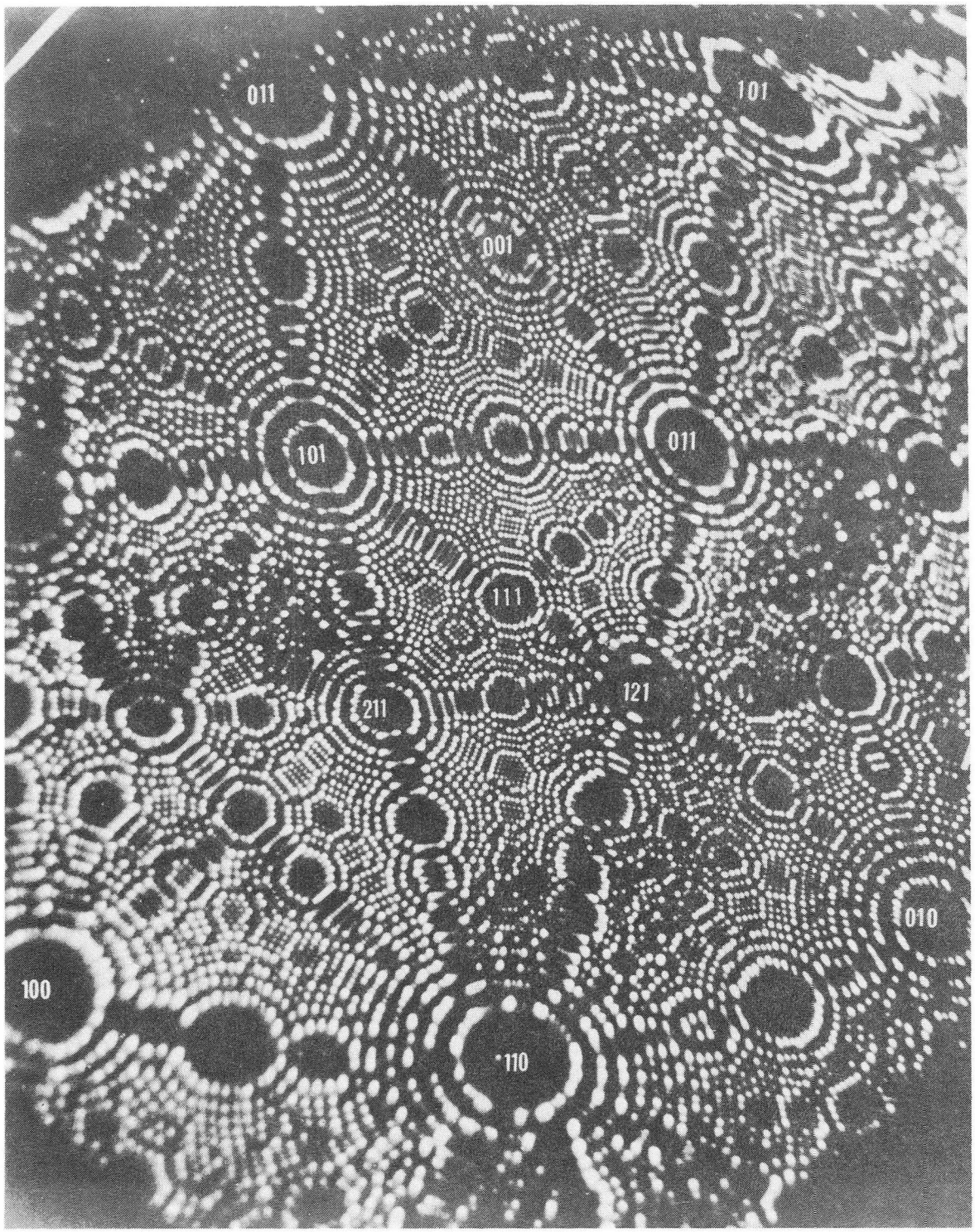

XBB 715-1883

Fig. 9

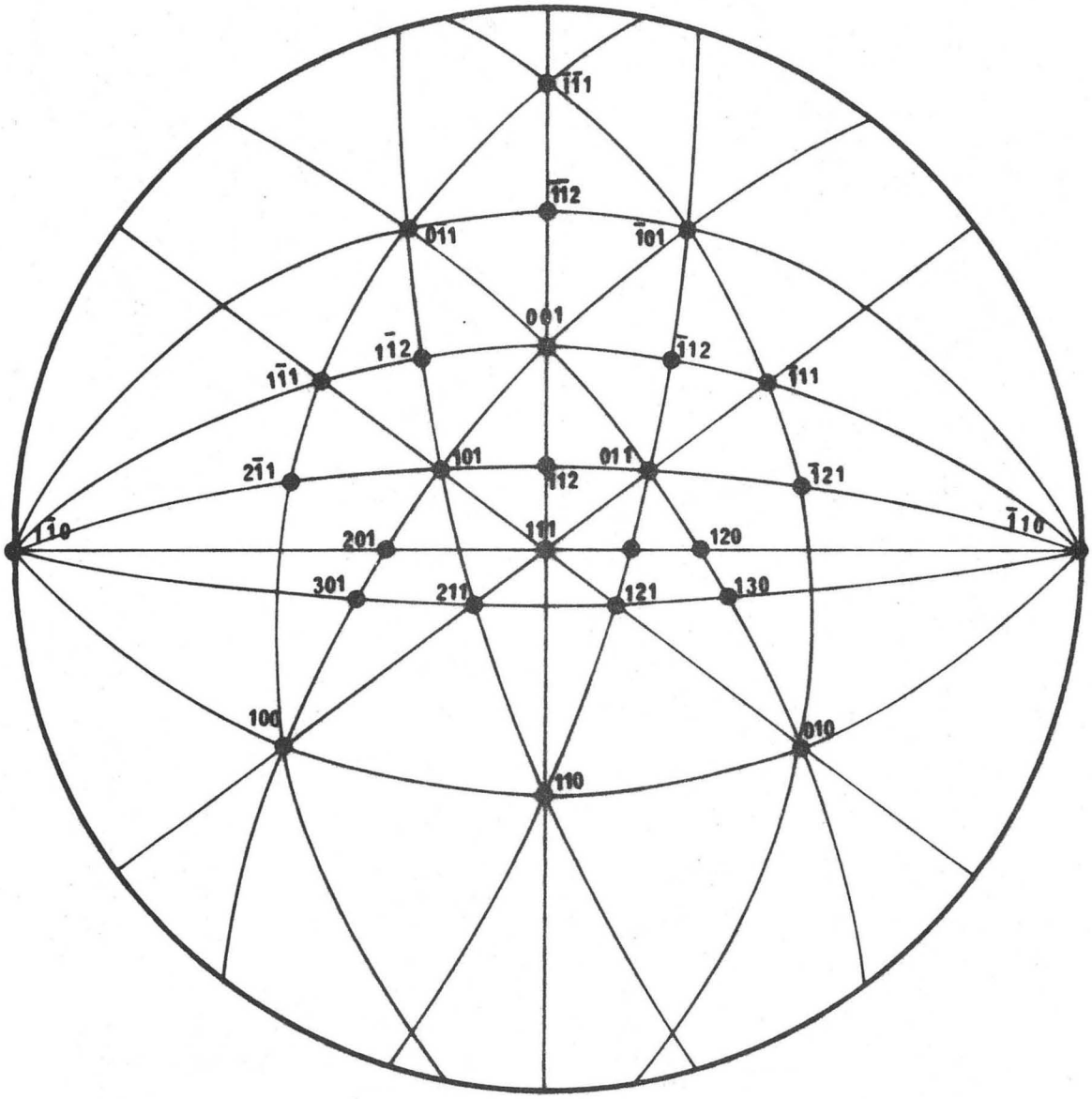

XBL708-3627

Fig. 10

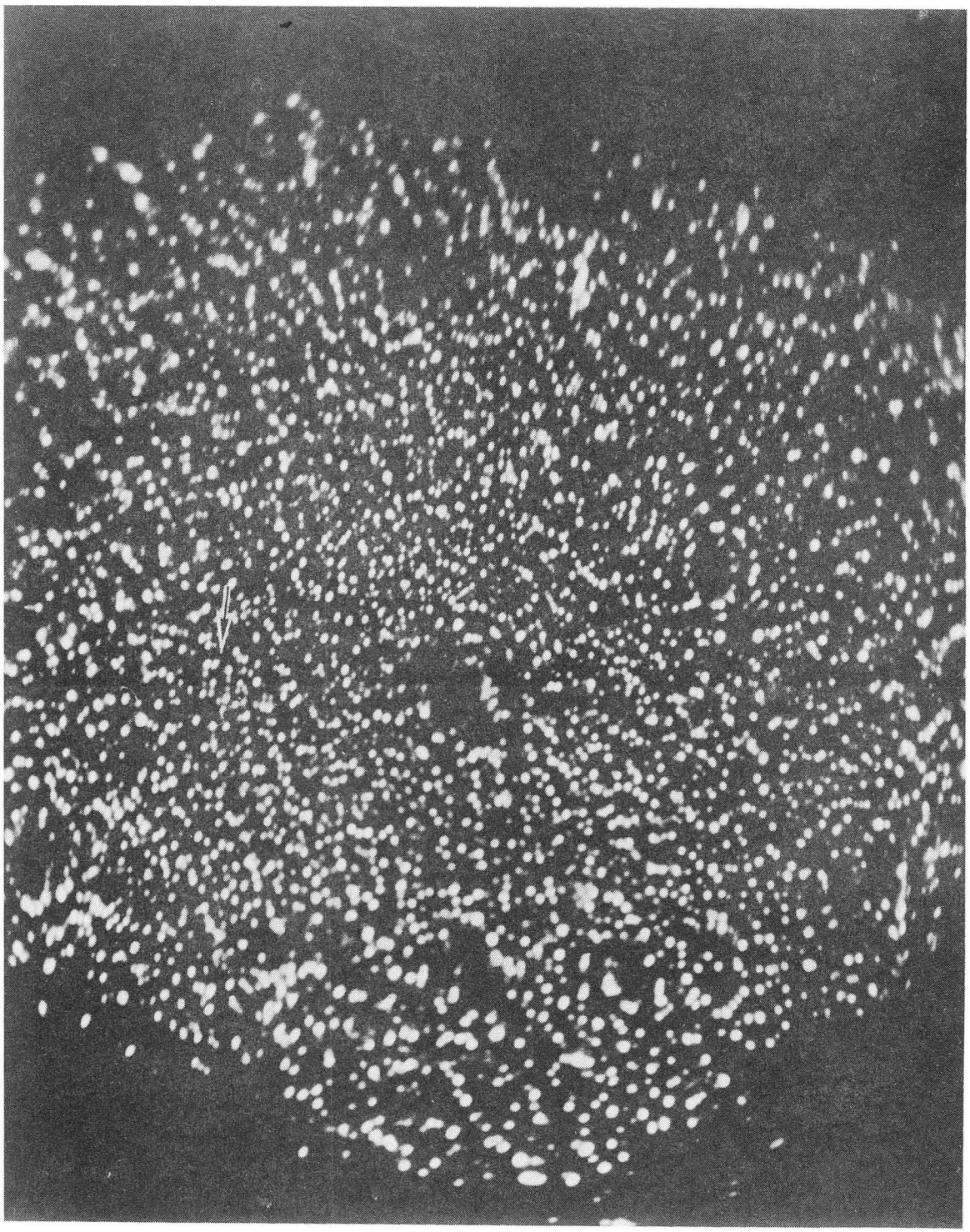

XBB 715-1891

Fig. 11a

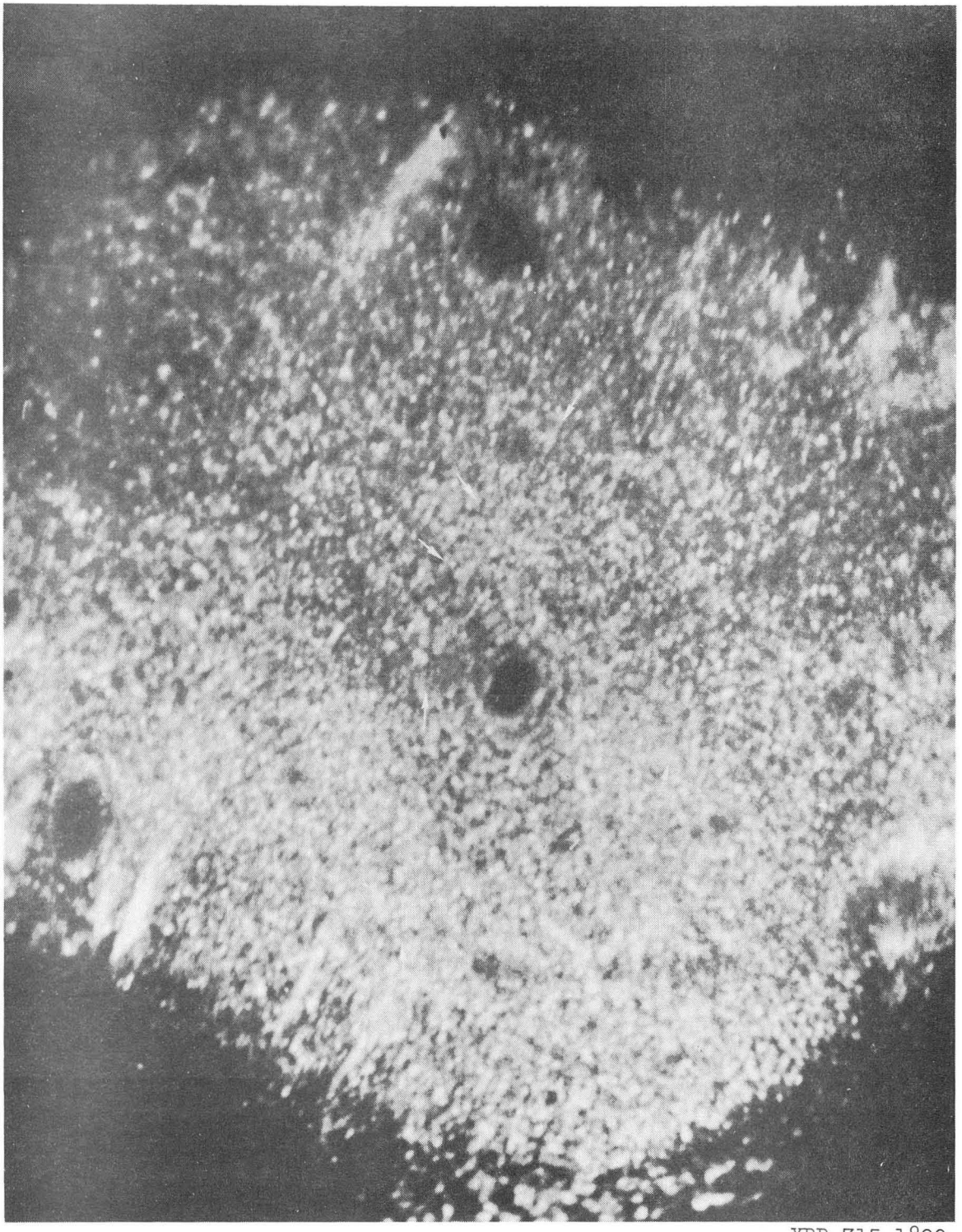

XBB 715-1890

Fig. 11b

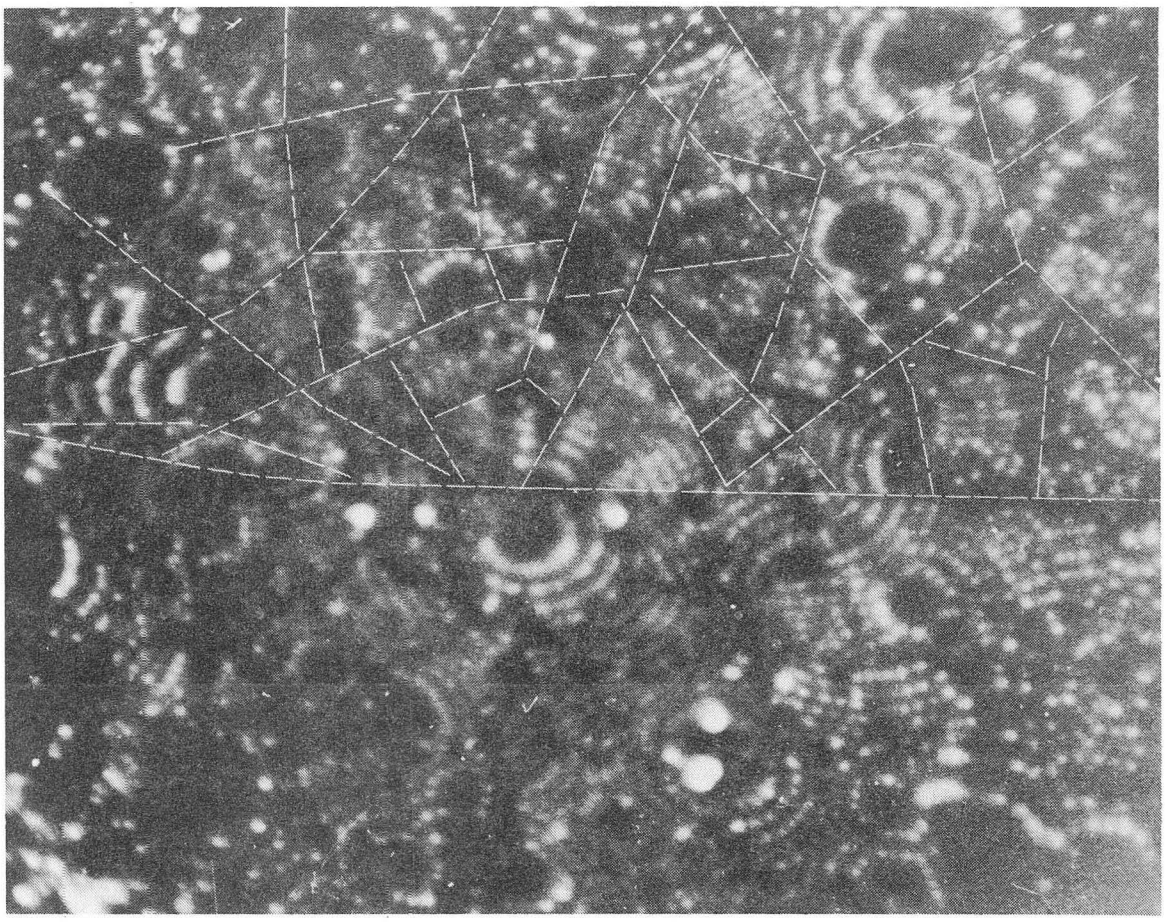

XBB 715-1892

Fig. 12a

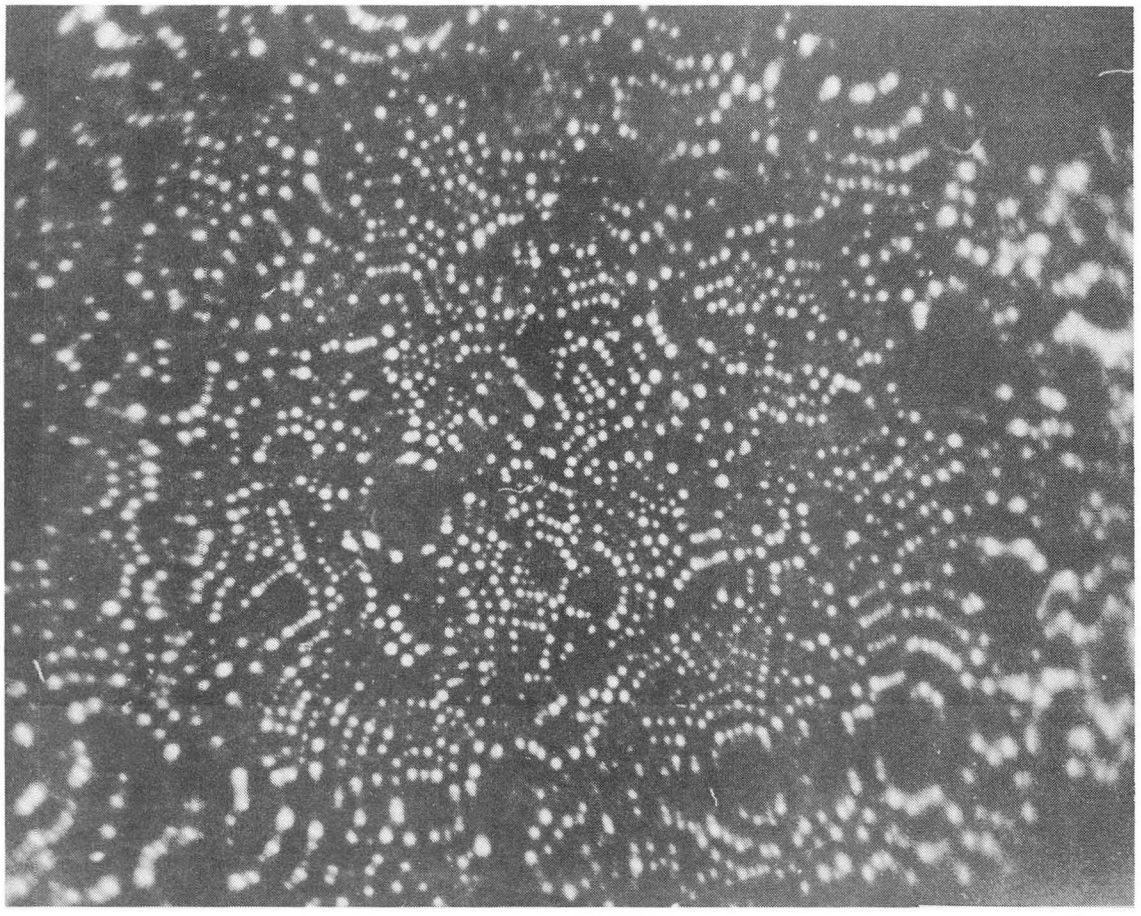

XBB 715-1895

Fig. 12b

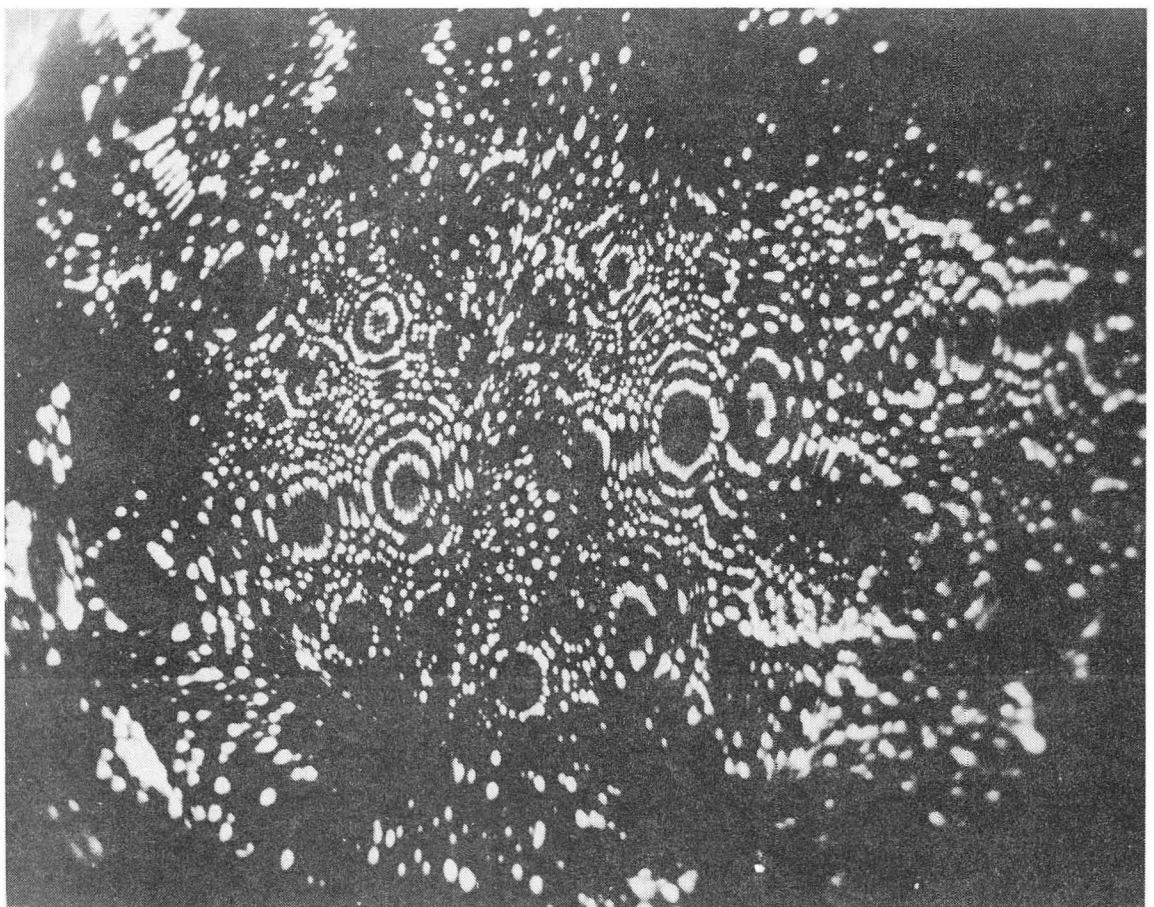

XBB 715-1893

Fig. 13a

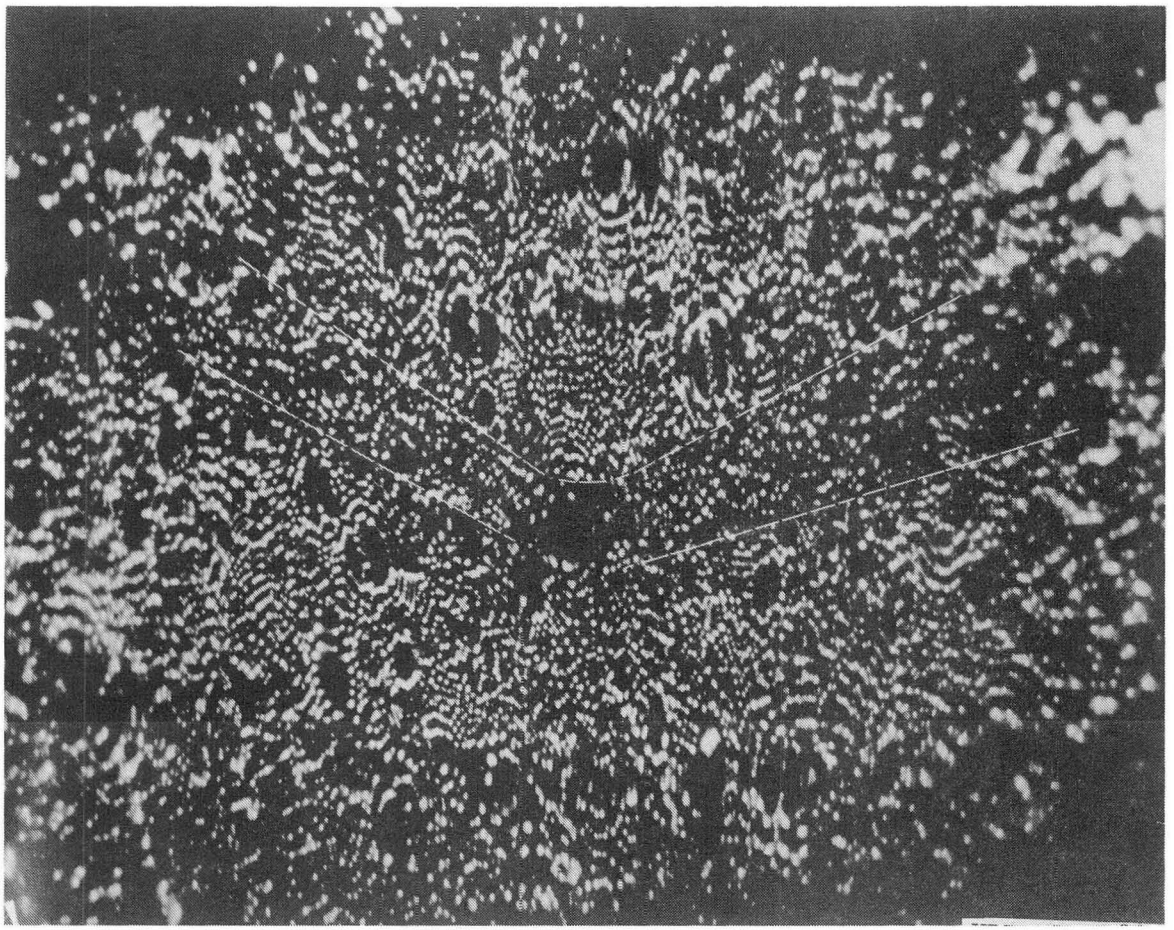

XBB 715-1881

Fig. 13b.

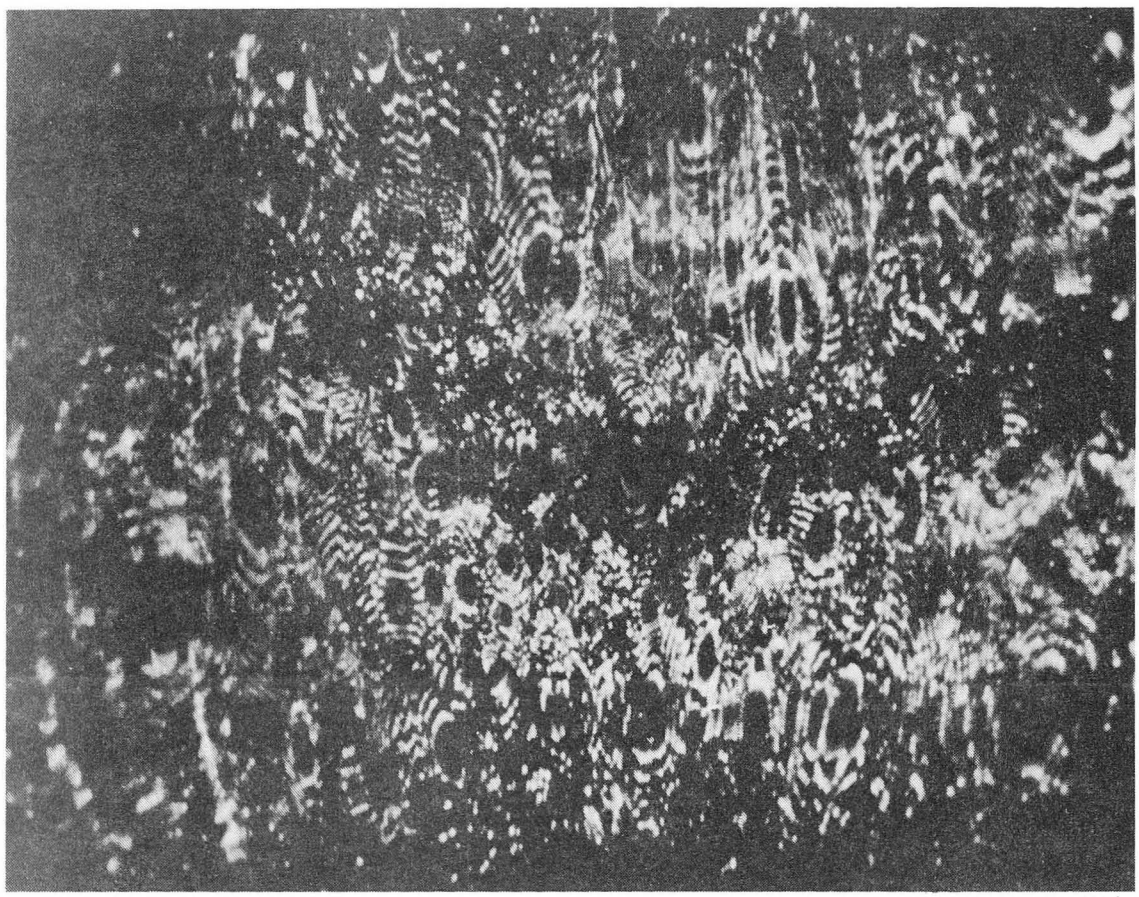

XBB 715-1894

Fig. 13c

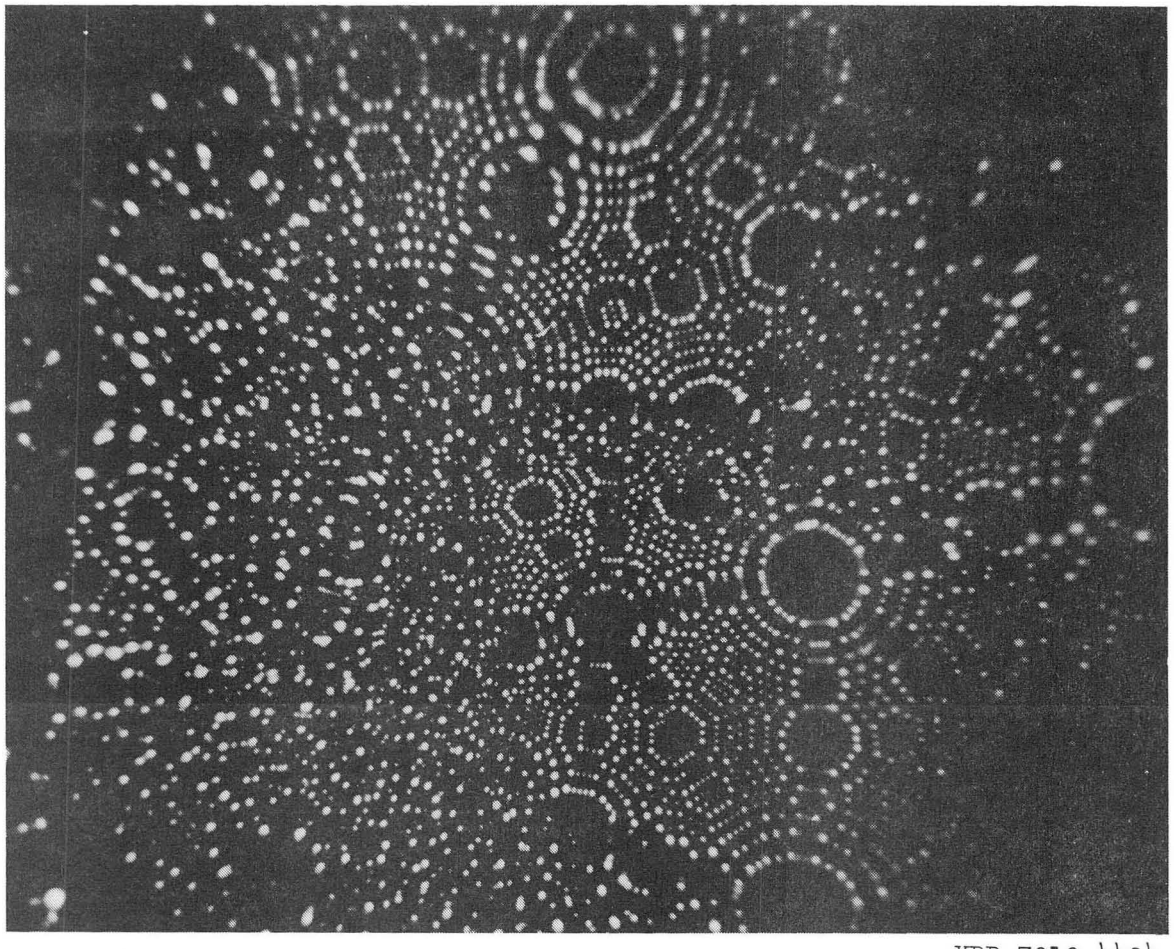

XBB 7010-4494

Fig. 14

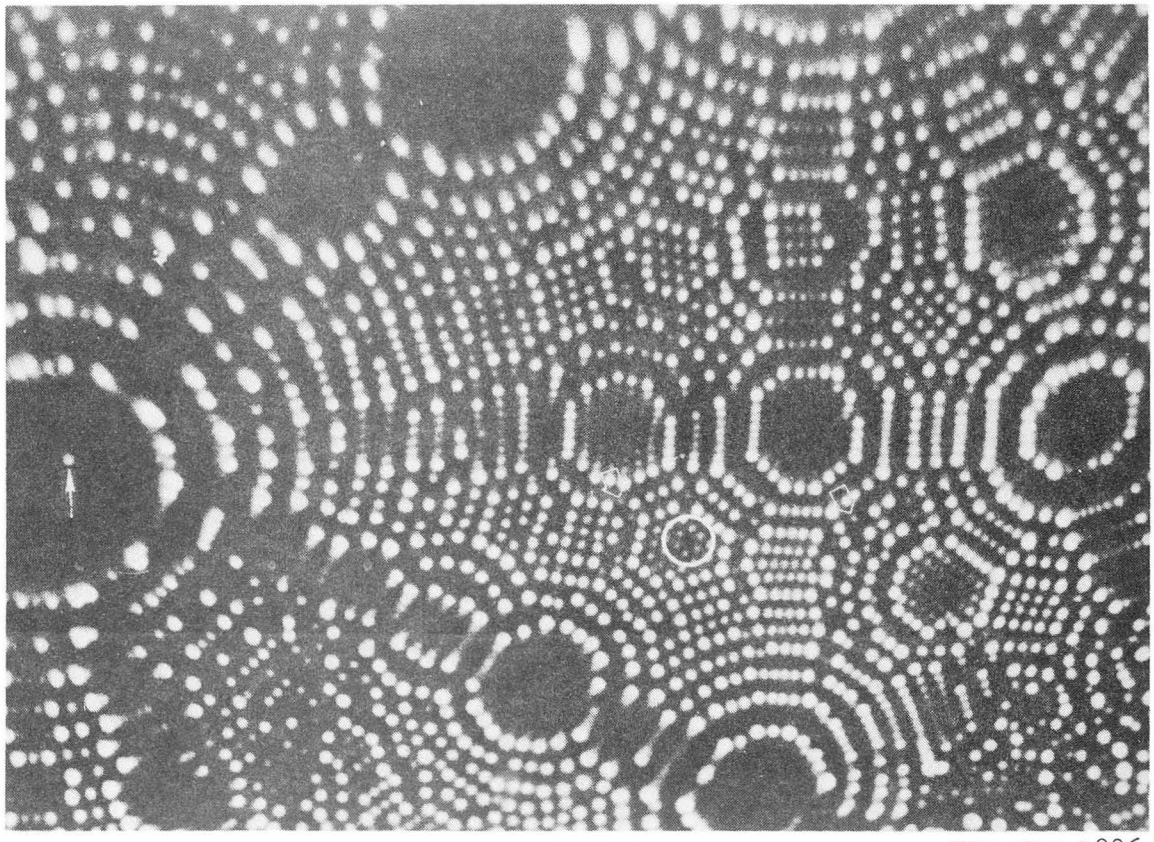

XBB 715-1886

Fig. 15

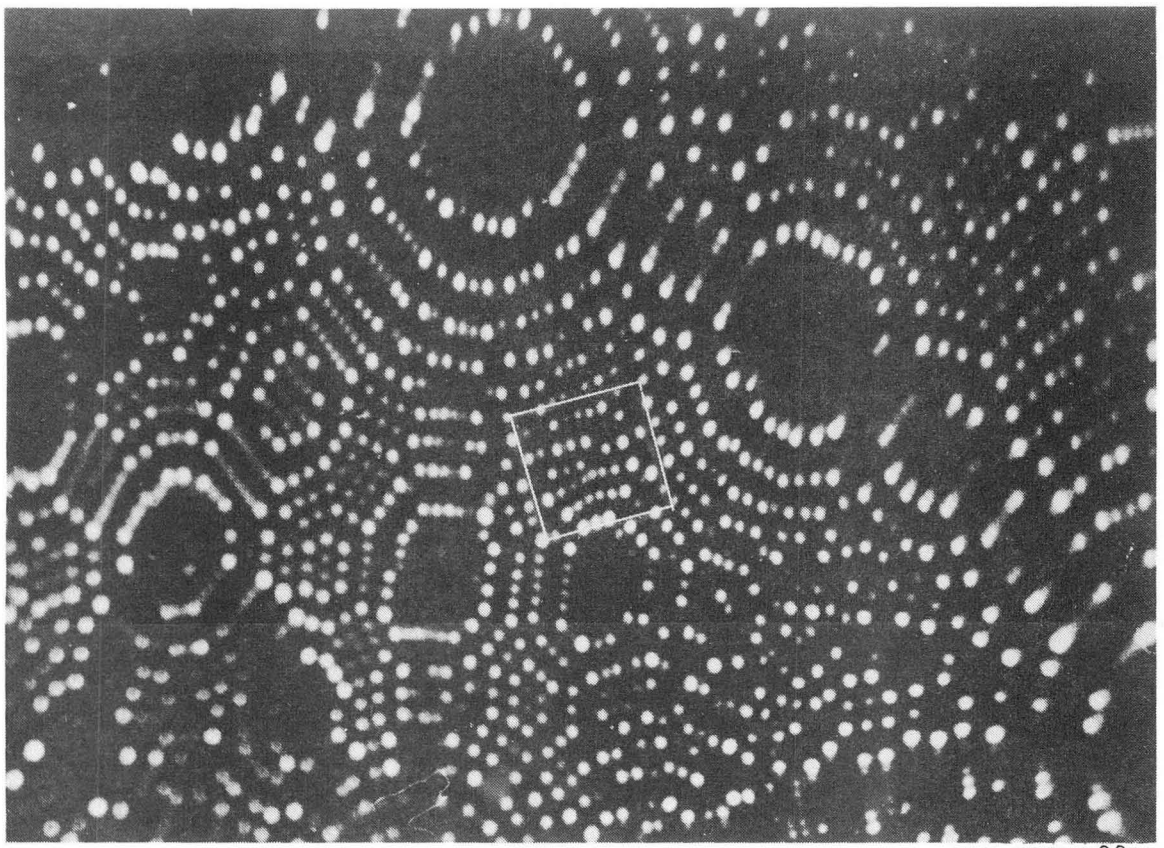

XBB 715-1885

Fig. 16

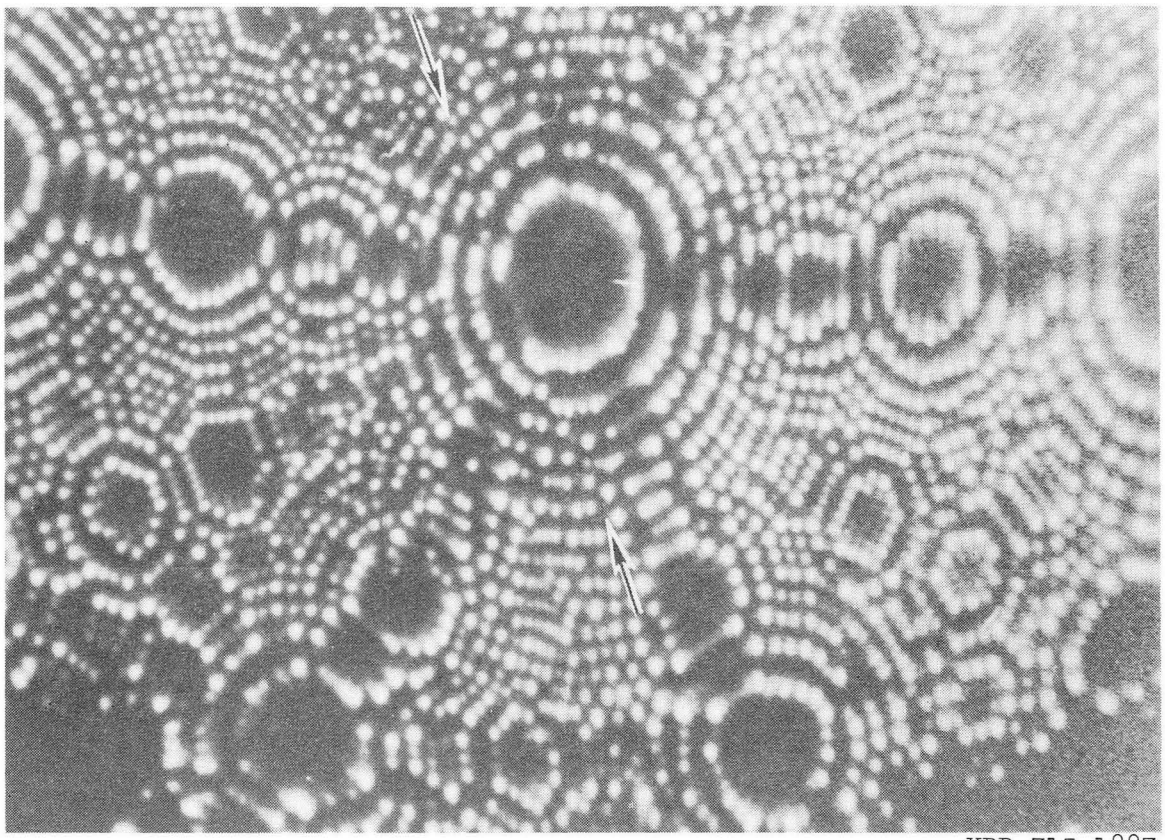

XBB 715-1887

Fig. 17

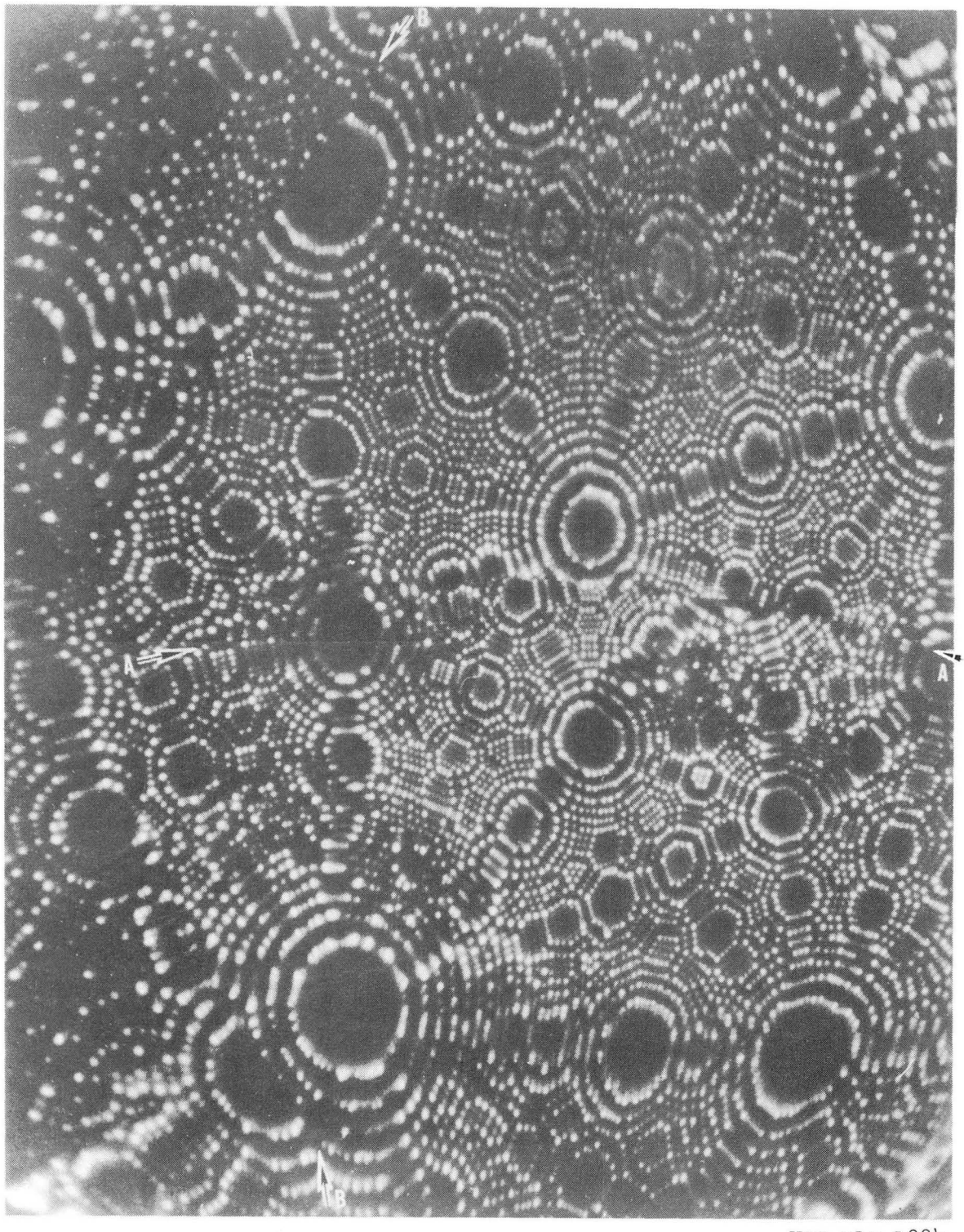

XBB 715-1884

Fig. 18

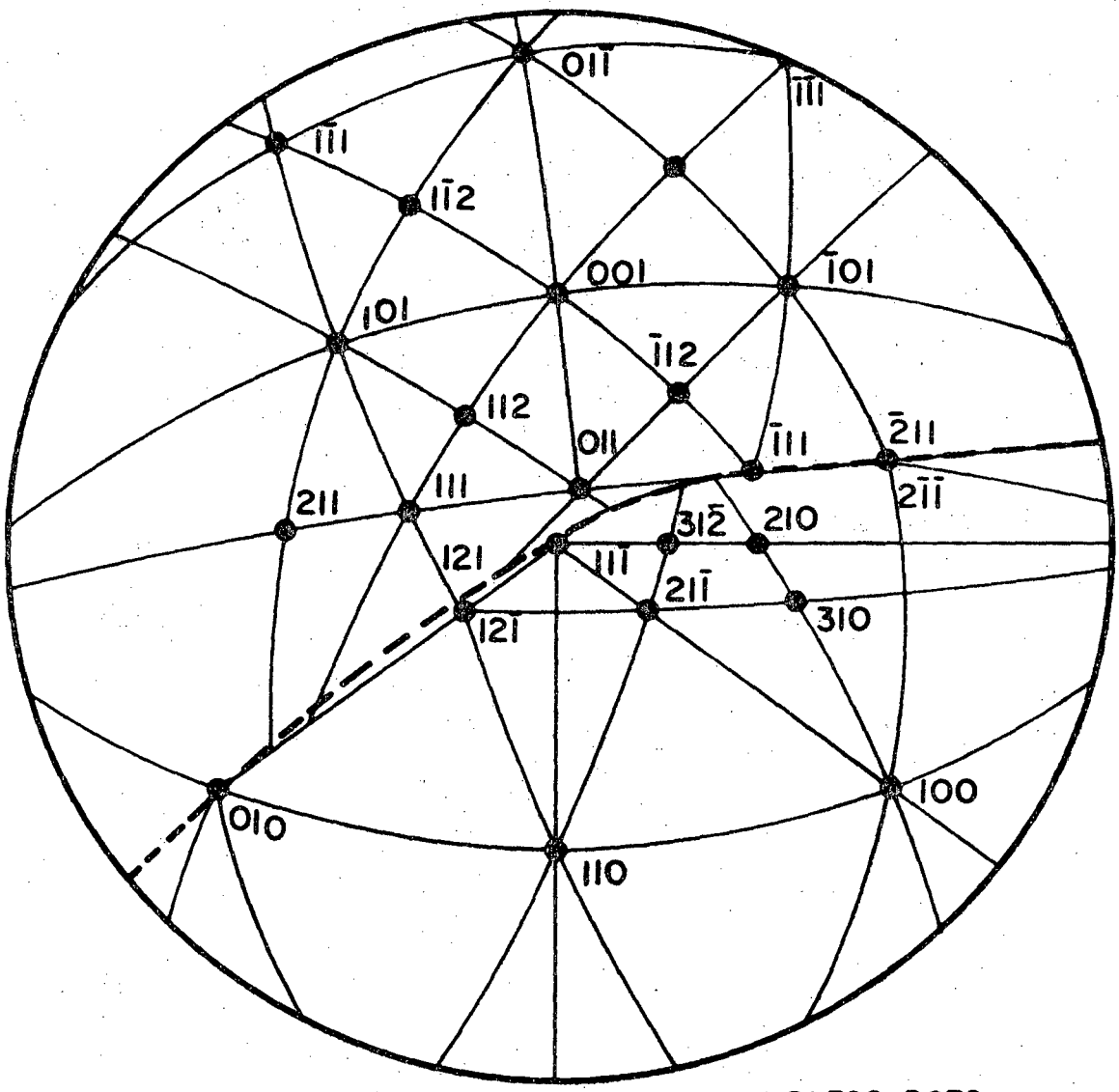

XBL708-3670

Fig. 19

LEGAL NOTICE

This report was prepared as an account of work sponsored by the United States Government. Neither the United States nor the United States Atomic Energy Commission, nor any of their employees, nor any of their contractors, subcontractors, or their employees, makes any warranty, express or implied, or assumes any legal liability or responsibility for the accuracy, completeness or usefulness of any information, apparatus, product or process disclosed, or represents that its use would not infringe privately owned rights.

TECHNICAL INFORMATION DIVISION
LAWRENCE BERKELEY LABORATORY
UNIVERSITY OF CALIFORNIA
BERKELEY, CALIFORNIA 94720